



The impacts of LULC and climate change scenarios on the hydrology and sediment yield of Rib watershed, Ethiopia

Lewoye Tsegaye · Rishikesh Bharti

Received: 19 July 2021 / Accepted: 12 August 2022 / Published online: 1 September 2022
© The Author(s), under exclusive licence to Springer Nature Switzerland AG 2022

Abstract Watershed-scale hydrology and soil erosion are the main environmental components that are greatly affected by environmental perturbations such as climate and land use and land cover (LULC) changes. The purpose of this study is to assess the impacts of scenario-based LULC change and climate change on hydrology and sediment at the watershed scale in Rib watershed, Ethiopia, using the empirical land-use change model, dynamic conversion of land use and its effects (Dyna-CLUE), and soil and water assessment tool (SWAT). Regional climate model (RCM) with Special Report on Emission Scenarios (SRES) and Representative Concentration Pathway (RCP) outputs were bias-corrected and future climate from 2025 to 2099 was analyzed to assess climate changes. Analysis of the LULC change indicated that there has been a high increase in cultivated land at the expense of mixed forest and shrublands and a low and gradual increase in plantation and urban lands in the historical periods (1984–2016) and in the predictions (2016–2049). In general, the predicted climate change indicated that there will be a decrease in precipitation in all of the SRES and RCP scenarios except in the Bega (dry)

season and an increase in temperature in all of the scenarios. The impact analysis indicated that there might be an increase in runoff, evapotranspiration (ET), sediment yield, and a decrease in lateral flow, groundwater flow, and water yield. The changing climate and LULC result in an increase in soil erosion and changes in surface and groundwater flow, which might have an impact on reducing crop yield, the main source of livelihood in the area. Therefore, short- and long-term watershed-scale resource management activities have to be designed and implemented to minimize erosion and increase groundwater recharge.

Keywords Climate change · Dyna-CLUE · LULC change · RCP · Scenario · Surface runoff

Introduction

Studies about runoff and sediment transport using timely data on hydrology, topography, predicted land use and land cover (LULC), and climate at watershed and catchment levels could be essential to designing and implementing catchment level resource management systems. The existence and competition for water will be altered as a result of LULC change and climate change, which will be induced by regional and global economic development (Luck et al., 2015). The rapid increase in LULC change, paired with climate variability, may result in substantial hydrologic effects (e.g., Chen & Yu, 2013).

L. Tsegaye (✉)
Department of Natural Resource Management, Bahir Dar
University, Bahir Dar, Ethiopia
e-mail: lewofrie@yahoo.com

R. Bharti
Department of Civil Engineering, Indian Institute
of Technology Guwahati, Guwahati, India

Spatially explicit empirical statistical models have been employed for predicting the locations of LULC changes (e.g., Irwin & Geoghegan, 2001; Lambin et al., 2000), which are vital for hydrologic studies. To develop precise projections of the forthcoming water balance, a comprehensive understanding of the dynamic land surface and its interacting parts is essential (Feyen & Raul, 2011). The alteration of rainfall-runoff and evaporation balances in watersheds could be because of LULC change due to anthropogenic activities (Kassa, 2009; Sahin & Hall, 1996). Factors such as institutions, demography, technology, biophysical elements, policies at regional and national scales, and macroeconomic activities can cause significant changes in LULC, which can affect hydrological systems at different spatial scales (Dibaba et al., 2020; Legesse et al., 2003). For studies related to land degradation and its effects on water resources, information on the extent, distribution, and types of LULC is a critical issue (Amsalu et al., 2007; Bewket, 2002). Land use information is essential in watershed hydrology, erosion, and sediment studies since it significantly affects hydrological processes of surface runoff, evapotranspiration, groundwater, streamflow, and sediment loads (e.g., Nie et al., 2011).

In order to execute appropriate water resource management plans, a practical understanding of the possible influence of LULC change on hydrologic variability is required (Stedinger & Griffis, 2008). Investigating the influence of LULC change on hydrology at the watershed scale allows for the identification of the degree of vulnerability of local water resources as well as the development of necessary mitigation measures that must be implemented ahead of time. Knowledge of LULC dynamics is vital to estimate future changes and support current and future sustainable management practices planned to preserve essential landscape functions (e.g., Lin et al., 2007).

Several researchers used LULC mapping tools and techniques to better understand LULC changes as well as changes in watershed hydrologic behaviors (e.g., Anand et al., 2018; Braimoh & Vlek, 2005; Houessou et al., 2013; Mango et al., 2011; Marhaento et al., 2017; Woldesenbet et al., 2017). The Rib watershed is among the Ethiopian highland watersheds that have been under frequent LULC conversions that impact the watersheds' hydrologic processes and soil erosion conditions. Water supplies in the Rib

watershed have been put under severe strain due to LULC change caused by the growing population and socio-economic developments. The Rib River's socio-economic importance, particularly to those living downstream of the watershed, as well as the effects of flooding and silt from the watershed to Lake Tana, are significantly affected by LULC changes. In this regard, Abe et al. (2018) and Dos Santos et al. (2018) reported that current and future LULC changes may jeopardize water supplies and hydrologic water balance, affecting the local communities, the biota, and water management plans of a basin directly. Integrated methodologies of hydrologic modeling and statistical methods on LULC alterations have not been well investigated to determine the effects of anthropogenic activities on the hydrological regime of the Rib watershed. Understanding and predicting the trends of the LULC changes while incorporating area-specific fundamental LULC drivers is an asset for hydrologic and soil erosion studies and designing and implementing sustainable management schemes in the Rib watershed.

There are numerous effects of climate change on hydrology that impact the water supply systems. Due to future climate change worldwide, there will be more drought and flood events with increasing intensity and frequency (Tebaldi et al., 2006). As global studies have shown, there is substantial variability in precipitation (increases and decreases by about 20%) in the twenty-first century (Bates et al., 2008). Changes in temperature and rainfall patterns are commonly observed in many parts of the developing world, particularly in arid and semi-arid regions (Akbari et al., 2021; Collier et al., 2008; Matata et al., 2019; Scholes, 2020; Serdeczny et al., 2017). The IPCC (2007) reported that the developing world is expected to suffer the most from the negative impacts of climate change and climate variability. Bates et al. (2008) reported that Africa is among the vulnerable continents to climate change and its average temperature increase is faster than the world average and has the tendency to continue in the future. Great spatial variation in precipitation was reported in Africa (a range between -13 and 57%) (Strzepek & McCluskey, 2006) and rise and drop between 25 and 50% in East Africa (Faramarzi et al., 2013). The high spatial variability of rainfall in Africa has resulted in variation in water availability. Ethiopia is vulnerable to climate change (Conway & Schipper, 2011). A

decrease in rainfall and an increase in temperature in Ethiopia have been reported in different studies. Funk et al. (2005), Fazzini et al. (2015), and Borgomeo et al. (2018) reported that Ethiopia's rainfall is expected to decrease in the future. As explained by the Ethiopian National Metrology Agency (ENMA, 2007), the future mean annual temperature will vary within the ranges of 0.9–1.1 °C, 1.7–2.1 °C, and 2.7–3.4 °C by 2030, 2060, and 2090 time slices respectively in Ethiopia.

Climate change's predictive effects on water availability for agriculture and industries have been researched to develop adaptive water management strategies (D'oll et al., 2015). In order to adopt proper climate adaptation measures, it is necessary to examine the future and existing implications of the changing climate on water and agriculture (FAO-IPCC, 2017). Climate change impacts on hydrology and sediments must be assessed before implementing effective methods to reduce its effect on water resources, land, and soils (IPCC, 2014). It is critical to conduct such a study in agro-ecological regions since the impact of climate change may be highly variable in different places. In this regard, GCM-derived climate change scenarios are frequently used to investigate the effects of climate change on hydrologic components (e.g., Abdo et al., 2009; Fowler et al., 2007; Hyandye et al., 2018; Subash et al., 2016).

The joint effects of climate change and dynamic LULC change on the accessibility of water are amplified by the fast-expanding population, putting strain on water resources and jeopardizing nations' food and water security. Climate change and spatio-temporal LULC data have a significant contribution to water management activities (e.g., FAO-IPCC, 2017). Land modification and climate change-related impacts on water resources are a pressing issue in the Blue Nile basin because much of the population in the region is engaged in rain-fed agriculture (Taye et al., 2015). Since it is situated in the upper Blue Nile basin of Ethiopia, the Rib watershed is under the challenges faced by LULC and climate changes. The rapid growth of population, combined with the expanding cultivated fields and urbanization in the Rib watershed has resulted in large-scale LULC changes. Furthermore, the pressure on the water resource of the Rib watershed is mounting due to the socioeconomic advancements and the recently higher demand for water downstream for rice cultivation.

Moreover, Lake Tana, which is the origin of the Blue Nile River, has been experiencing a high rate of sedimentation from the Rib River watershed as a result of the impacts of poor land management, frequent LULC changes, and climate change (Setegn et al., 2011). Because agriculture is the main source of income for the overwhelming majority of Ethiopians, including the study watershed, frequent land conversion, and the related land degradation is a serious agenda. Land-use change is a rapid and continual process that necessitates a comprehensive investigation of its predictive trends and the likely impacts on hydrology and soil erosion. There is a considerable gap in land use prediction incorporating their driving factors in Ethiopia and in the Rib watershed. Impact studies in Ethiopia rely on LULC data from the past, making it impossible to predict the future effects of changing land use on hydrological components. An important contribution related to this is an adequate approach for projecting future scenarios of land uses by integrating physical and social factors of land-use changes. In this regard, investigating scenarios of land-use changes using the Dyna-CLUE modeling framework, which integrates the social and physical factors of change and which has not been practiced in the Ethiopian conditions, helps to understand the prospective effects of land use scenarios on the watershed hydrology and soil erosion and could provide a scientific basis to undertake predicted implications of LULC change in the highlands of Ethiopia, where land degradation and nutrient depletion are more severe than other regions in Africa. This study verified and validated that the Dyna-CLUE modeling framework is applicable in land use scenario modeling in the Ethiopian context. The analysis of the land use projection also contributed to the design and implementation of immediate and future long-term land management plans by considering the social and environmental factors of the land-use changes in the area.

There has been a significant gap in the scenario-based prediction of the implications of LULC and climate change on hydrology and soil erosion in Ethiopia. The LULC dynamics and climate change have had a huge impact on the Rib River watershed, which is the headwater and significant donor of water to the Nile River, potentially resulting in water stress in Nile riparian countries. Limited studies conducted to investigate the implications of LULC and climate change

on the hydrology upstream of the Blue Nile basin of Ethiopia were dependent on past LULC and climate change (e.g., Berihun et al., 2019; Rientjes et al., 2011) or past LULC and future climate change (e.g., Abdo et al., 2009; Adem et al., 2016; Alemseged & Tom, 2015; Setegn et al., 2011; Shiferaw et al., 2018; Worqlul et al., 2018) with an emphasis on GCM outputs of the third and fourth assessment reports of the IPCC for the future climate analysis. Rientjes et al. (2011) reported that there has been a decreasing trend in rainfall and an increasing trend in historical LULC change that has highly affected the streamflow of the upper Gilgel Abbay watershed in Ethiopia. A study by Worqlul et al. (2018) using the Hadley Center climate model (HadCM3) output in the Gilgel Beles and Main Beles watersheds of Ethiopia revealed that the minimum and maximum temperatures will increase by 3.6 °C and 2.4 °C, respectively, at the end of the twenty-first century, which might result in 64% and 19% increase and decrease in streamflow in wet and dry seasons, respectively. In this study, predicted scenarios of LULC and climate change were analyzed to examine the future status of the hydrology and sediment yield of the Rib watershed. The study analyzed and compared the GCM-RCM model outputs of climate scenarios from the fourth assessment reports and RCPs, which was not the case in previous studies in Ethiopia, to evaluate the predictive implications of climate change on hydrology and sediment outputs.

Moreover, impact studies in the Ethiopian highlands lack a comprehensive analysis of the effects of LULC and climate change on sediment loss, which is the country's most critical problem. This study analyzed and predicted the erosion and sediment loss, which is the critical problem of land degradation and loss of agricultural yields in the Rib watershed due to climate and LULC changes. Most notably, no previous study about the impacts of LULC and climate change scenarios on hydrology and sediment yield has been undertaken in the study watershed, which provides a considerable amount of water and sediment to Lake Tana, the source of the Blue Nile River. Therefore, the objectives of this study were to assess the impacts of future climate changes (FCC) and joint impacts of future LULC changes (FLULCC) and (FCC) on the hydrology and sediment yield of the Rib watershed on a monthly, seasonal, and annual

basis from 2025 to 2099. The knowledge and practice of this study provide insight for policymakers to focus on policy options that could mitigate the impacts of the changing climate and land uses and also assist watershed managers to plan and implement proper soil and water management methods to reduce erosion and augment water resources in the study watershed and neighboring watersheds in the highlands of Ethiopia.

Description of the study area

The Rib watershed is part of the Northwestern highlands of Ethiopia and is located between 11° 42' 34"–12° 13' 45" N and 37° 36' 6"–38° 14' 20" E (Fig. 1). The size of the watershed is about 1293.2 km², and its elevation varies between 1786 and 4098 m AMSL. Mount Guna is one of the high mountain ranges in Ethiopia, and its peak, around 4135 m AMSL, is the origin of the Rib River. The mouth of the river is Lake Tana, which is the largest lake in Ethiopia and among the largest in Africa. The watershed is hilly and undulating in its upstream and flat plain downstream, which leads to frequent flooding. There is a main rainy season locally known as "Kiremt" from June to September and an intermediate season that has minor rains between April and May known as "Belg." The dry season is known as "Bega," which prevails from October to February. The rainfall distribution is unimodal, with the highest amount in July, August, and September. The watershed has a highland type of climate with an annual rainfall of about 1379 mm. Its annual average temperature is about 21.4 °C, and the high temperature (24.5 °C) is recorded during the Belg season (March to May). The watershed is dominated by a huge volcano system named Guna Mountain shield volcano. The common rock type for this material is basalt with intruded and overflowed lava, volcanic ash, and other acidic rocks. Silt to clay deposits dominate the downstream of the watershed due to flooding by the river (MoWR, 1998). The main soil types of the area are Vertisols, Leptosols Fluvisols, Luvisols, and Nitosols. The dominant land uses include cultivation, grazing, shrubs forests, and settlement (BoEPLAU, 2015).

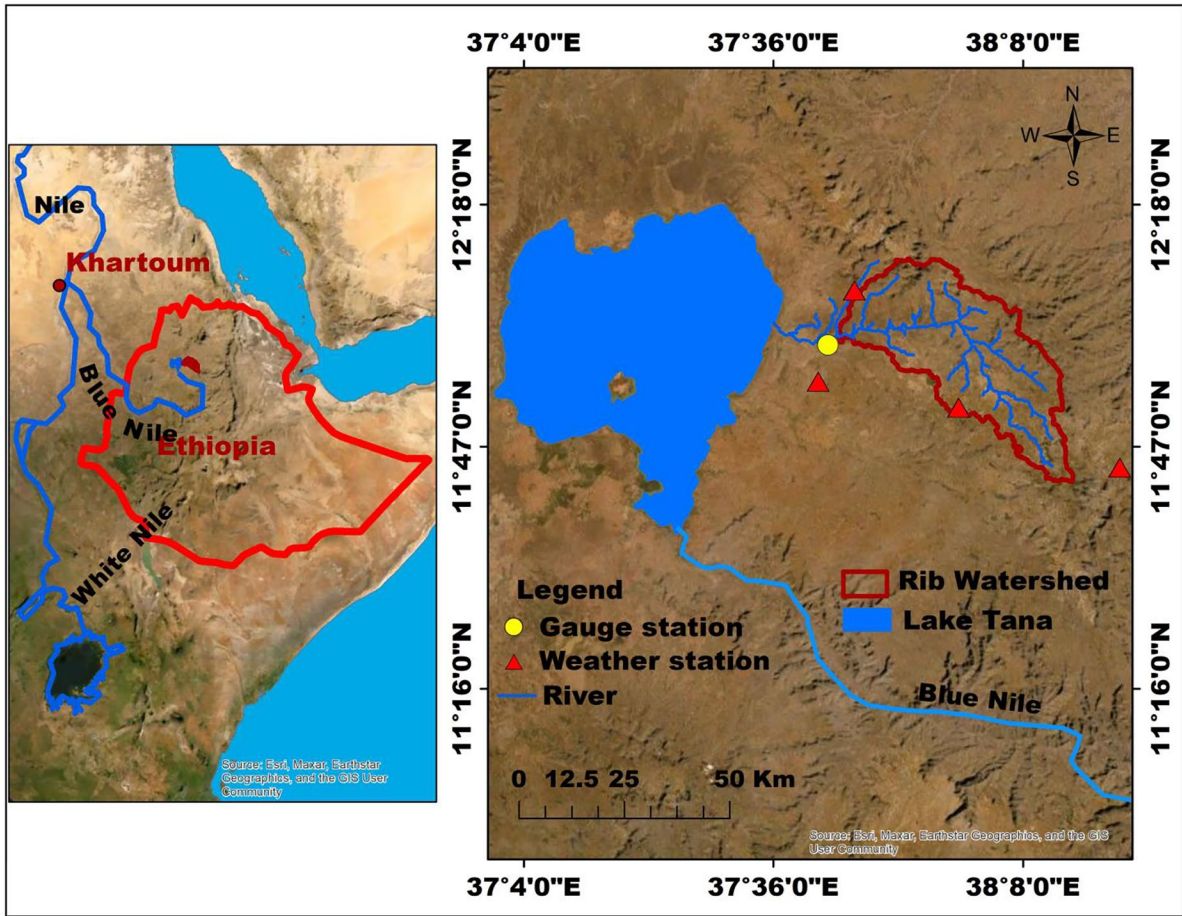


Fig. 1 Location map of the study area

Materials and methods

Data and methodology

Data

A Shuttle Radar Topography Mission (SRTM)-derived Digital Elevation Model (DEM) of 30 m×30 m resolution for slope classification, watershed, and HRU delineation was acquired from the USGS website (<https://earthexplorer.usgs.gov/>). The soil types and physicochemical properties for the requirements of the SWAT model were obtained from the Abbay Basin Integrated Master Plan Project of the Ministry of Water Resources of Ethiopia (MoWR, 1998). Additional physicochemical properties of the soils were also obtained from the Bureau of Environmental

Protection, Land Administration and Use (BoEPLAU, 2015) and a digital soil map of the world at <http://www.fao.org/geonetwork/srv/en/metadata.show?id=14116>. Supervised classification was conducted on a 30-m-resolution LANDSAT 5, 7, and 8 images acquired in March 1984, 2003, and 2016, using Thematic Mapper (TM), Enhanced Thematic Mapper (ETM), and Operational Land Imager (OLI) sensors, respectively (Table 1) to prepare the LULC data for the setup of the SWAT model, preparing land use demand, and land use predictions. The LULC map of 2016 was used as a base map for the setup of the SWAT model. The images were directly downloaded from the USGS website at <https://earthexplorer.usgs.gov>. The meteorological data (precipitation, temperature, solar radiation, wind speed, and relative humidity) from 1990 to 2016 were acquired from the National Meteorological Agency of Ethiopia

Table 1 Satellite images and their properties for the LULC classification

Satellite	Sensor	Acquisition date	Spatial resolution	Path and row
LANDSAT 5	TM	15 Mar 1984	30 m	169/52
LANDSAT 7	ETM	08 Mar 2003	30 m	169/52
LANDSAT 8	OLI-TIRS	04 Mar 2016	30 m	169/52

(NMA), and the data were analyzed and arranged to suit the SWAT model. Streamflow and sediment data from 1990 to 2016 were obtained from the Ministry of Water Resources of Ethiopia (MoWR) for the ArcSWAT calibration and validation.

The hydrology model (SWAT) and impact assessment

The hydrologic model, soil and water assessment tool (SWAT), is physically based, semi-distributed, effective in continuous simulation for longer periods of time, and computationally efficient (Arnold et al., 1998, 2012; Gassman et al., 2007). Groundwater flow, evapotranspiration, surface runoff, lateral flow, tributary channels, return flow, canopy storage, and infiltration are the key hydrological components modeled under the land phase of the hydrology cycle in the SWAT model. Since it considers geographic and temporal variability based on multiple possible physical factors, SWAT is capable of estimating sediment output at catchment scales generated through surface flow, gully, and channel erosion. The model provides better sympathy for the processes of sediment transport and deposition due to overland flows. Channel network transport of sediments is the result of the processes of degradation and aggradation (Neitsch et al., 2005) and the HRU level sediment yield in the SWAT model is estimated using the Modified Universal Soil Loss Equation (MUSLE) (Williams, 1975).

The ArcSWAT model setup comprises the LULC map derived from the LANDSAT image acquired in March (dry season) 2016, as well as meteorological, soil, and topographic (DEM) data. The watershed and a total of 37 sub-watersheds with an area variation between 67.7 and 10,769.5 ha were delineated using the 30×30-m DEM. Through its HRU analysis, SWAT performs HRU delineation by superimposing

spatial data of soil, slope, and land use. The smallest spatial extent in the SWAT model is the HRU, which embraces unique soil type, land use, and slope classes. An HRU-based analysis of the SWAT model helps to discriminate the spatial variations in a basin or watershed, which is a fundamental input for watershed management interventions. With unique combinations of land use, soil, and slope classes, a total of 420 HRUs were defined for the Rib watershed. The software package of the SWAT calibration and uncertainty program (SWAT-CUP) (Abbaspour, 2013) was used to calibrate the model using flow and sediment data from 1993 to 2007, which was collected from the gauge station of the watershed. The warm-up period for the calibration was from 1990 to 1992, and the data for validation was from 2008 to 2016, as is presented in the “Results” and “Discussion” sections of “Sensitivity analysis, calibration, validation, and performance evaluation of the SWAT.” The calibrated model is used to predict the hydrology and sediment yield of the watershed. The future impact assessment was analyzed from 2025 to 2099 in time slices of 2025–2050, 2051–2074, and 2075–2099. The impact assessment was estimated using two scenarios: future climate change and future LULC change (FCC&FLULCC), and future climate change (FCC), to differentiate the impact of LULC and climate changes. The climate is predicted for 2099, and the LULC is for 2049 for the impact analysis.

Sensitivity analysis, calibration, validation, and performance evaluation in SWAT

Since the SWAT model has a lot of sediment and flow parameters, it is important to figure out which ones are the most sensitive to improve the model’s calibration. The influence of a set of characteristics on estimating total flow and sediment was determined using sensitivity analysis, a technique for determining the response of a set of parameters. The degree of change in output parameters in relation to the model’s input parameters is checked using the sensitivity analysis. The sensitivity analysis, calibration, and validation were processed using the Sequential Uncertainty Fitting (SUFI-2) incorporated in the SWAT-Calibration and Uncertainty Program (CUP) (Abbaspour et al., 2015) using measured flow and sediment data obtained from the Rib watershed outlet. A calibration is an approach to adequately parameterizing the model to a particular

set of local conditions in order to minimize the prediction uncertainty (Moriassi et al., 2007). This procedure entails comparing simulation findings to datasets of observed streamflow and sediment outputs. Monthly flow and sediment outputs were calibrated for 15 years (1993–2007) and validated for 9 years (2008–2016) with a 3-year warm-up period (1990–1992). Validation is the procedure of ensuring that the model is capable of producing a fairly accurate simulation. To evaluate the appropriateness of the model for the simulations, the observed and predicted values are compared.

The fitness of simulations with observations of streamflow and sediment data was evaluated using statistics suggested by (e.g., Moriassi et al., 2007) such as percent bias (PBIAS), Nash–Sutcliffe efficiency (NSE), coefficient of determination (R^2), and the ratio of the root-mean-square error to the standard deviation of measured data (RSR). Model performance rates were based on the Moriassi et al. (2007) statistics, where R^2 ranges from 0 to 1, with a higher value indicating less inaccuracy. The NSE varies from infinity (inaccuracy) to one (best). A PBIAS value of near 0 represents the best prediction, whereas negative and positive values indicate model overestimation and underestimation, respectively. RSR can range from 0 to a very large positive number, where a better model simulation is represented by lower values. The performance statistics were computed using Eqs. (1) through (4).

$$R^2 = \left[\frac{\sum_{i=1}^N (O_i - \bar{O})(S_i - \bar{S})}{\sqrt{\sum_{i=1}^N (O_i - \bar{O})^2} \sqrt{\sum_{i=1}^N (S_i - \bar{S})^2}} \right]^2 \tag{1}$$

$$NSE = 1 - \frac{\sum_{i=1}^N (O_i - S_i)^2}{\sum_{i=1}^N (O_i - \bar{O})^2} \tag{2}$$

$$PBIAS = 100 \frac{\sum_{i=1}^N (O_i - S_i)}{\sum_{i=1}^N O_i} \tag{3}$$

$$RSR = \frac{RMSE}{STDE_{obs}} = \frac{\left[\sqrt{\sum_{i=1}^n (O_i - S_i)^2} \right]}{\left[\sqrt{\sum_{i=1}^n (O_i - \bar{O}_i)^2} \right]} \tag{4}$$

O_i and S_i are the measured and projected values, respectively, in the equations above. N represents the number of observations, and the mean of measured and model-simulated values are represented by \bar{O} and \bar{S} , respectively.

The 95% probability distribution, computed from the 2.5% to 97.5% levels of cumulative distributions of variables in the output, is used to represent the propagation of uncertainty in model outputs in SUFI-2 (Abbaspour et al., 2015). The fit between the 95% prediction uncertainty (95PPU) results and the observations is quantified with the statistics of the P-factor and R-factor. The P-factor refers to the proportion of observations covered by the 95PPU, which ranges from 0 to 1, with 1 being the best value, while the R-factor refers to the thickness of the 95PPU with its best value near 1.

Land use land cover data and accuracy assessment

The data required for the Dyna-CLUE model are land use, drivers of change, demand for land-use change, and land-use type-specific conversion settings. Historical remotely sensed imageries were used in land use modeling research to define transition parameters across landscapes (e.g., Conway & Lathrop, 2005; Theobald & Hobbs, 2002). The trend-based modeling methodology is based on the assumption that future land-use trends would be comparable to recent historical trends (Theobald & Hobbs, 2002). A 30-m-resolution LANDSAT 5, 7, and 8 images acquired in March 1984, 2003, and 2016 using TM, ETM, and OLI sensors respectively were used to classify the LULC maps. After implementing an image processing technique of histogram equalization to improve contrast on the LANDSAT images, a supervised image classification method using a maximum likelihood algorithm was conducted to categorize pixels into 1984, 2003, and 2016 LULC classes (grassland, mixed forest, plantation, shrubland, intensively cultivated, moderately cultivated, urban, and waterbody). The LULC maps were used to prepare the land-use demands of the watershed to predict the LULC scenario map for 2049. For the accuracy assessment, ground control points (GCPs) were collected from the field, and discussions were held with aged people living in the locality to identify the covers in the historical images. A total of 547, 505,

and 553 GCPs were collected in 2019 for the accuracy assessment of 1984, 2003, and 2016 classified images, which have an area size of 129,323.61 ha or 1293.2 km². The kappa coefficient and error matrix (Lillesand & Kiefer, 2004) classification accuracies were calculated through a GIS overlay of the thematic classified images and the GCPs.

The kappa statistics values range between 0 and 1 (complete agreement) and are multiplied by 100 to obtain their percentage. The strong agreement (> 0.80 (80%)) and high agreement (0.60–0.80 (60 to 80%)) values of Kappa (Congalton & Green, 1999) indicate a better relationship between the classified images and the reference data (Table 2). The 1984 LULC was used as a base map for the LULC modeling. ASCII files for each land use type were prepared for the land-use prediction modeling.

Prediction of LULC changes

The LULC changes were projected using the Dyna-CLUE model (Verburg & Overmars, 2009). It predicts future land-use change using empirically calculated relations between driving factors and land uses. In modeling land-use change, the Dyna-CLUE considers the internal competition among land uses. The model was established for use on continental and national scales. The Conversion of Land Use and its Effects at Small Regional Extent (CLUE-S) (Verburg et al., 2002) was later developed into Dyna-CLUE versions at Wageningen University by Verburg and Overmars (2009). The Dyna-CLUE has four components: land-use requirements, location characteristics, spatial policies and restrictions, and sequences of land-use conversions (Verburg & Veldkamp, 2004; Verburg et al., 2002). The Dyna-CLUE model is based on the idea that observable spatial relationships between land-use types and putative driving factors represent active processes that will continue to exist in the future. As a result, the model could not capture changes in driving factors over time (Tizora et al., 2018; Wang et al., 2019; Zhang et al., 2013).

Land use demand, sequence of land-use conversions, and conversion elasticity

Land use demand is the planned land-use size assigned to each land-use category in each of the study years. The most prevalent method for analyzing land-use

demand is trend extrapolation from the recent past into the near future (Verburg, 2010). The historic land uses of 1984, 2003, and 2016 were used for the trend extrapolation to prepare the land-use demand of this study. Not all land uses are possible to change, but instead follow a certain sequence. Some land uses are very unlikely to change, e.g., arable land cannot be converted directly into the primary rainforest (Verburg & Overmars, 2009). In the Dyna-CLUE model, the land-use conversions that are possible and impossible are determined in a land-use conversion matrix, which is important to indicate to what land use types a defined land use is likely to convert. The conversion matrix in this study was determined using previous trends, i.e., analysis of changes between 1984 and 2016 (Tizora et al., 2018) and knowledge of experts and aged people in the locality. If the conversion is allowed, the value of 1 is assigned to the cell, and if not allowed, 0 is used instead (Verburg, 2010).

Conversion elasticity indicates the temporal dynamics of land uses and designates the reversibility of land-use changes. High capital-intensive land uses that could result in an irreversible impact on an area could not be easily converted to others. In the study, land-use types were assigned a dimensionless factor from 0 (easily convertible) to 1 (static to change) to indicate their relative elasticity to change based on expert knowledge and analysis of previous land use data in the locality. High elasticity was assigned to built-up and waterbodies, given their low probabilities of being converted to other land-use types, whereas low elasticity values were allocated to shrubland, forests, and grasslands due to their higher likelihood of conversion to other land-use types because of agricultural land expansion.

Driving factors of change and location suitability

Land-use changes are likely to occur in a grid cell that has a higher preference or suitability. The land-use preference is determined through the iteration procedure between land-use classes (dependent variable) and driving factors (independent variable) in the Dyna-CLUE model. The influential land-use driving factors specified for this study were population density (social factor), topography, soil depth, soil texture, distance to waterbody, roads, towns, and churches, rainfall, and temperature (physical factors) (Table 3). The stepwise binomial logit model

Table 2 Error matrix of the accuracy assessment of the classified images of 1984, 2003, and 2016

	0	1	2	3	4	5	6	7	Row total	User Acu%
Referenced 1984										
Classified 1984										
0	134	3	–	–	11	–	1	2	151	88.7
1	–	83	10	3	–	1	–	–	97	85.6
2	4	2	63	–	4	–	–	–	73	86.3
3	–	9	1	40	–	2	–	–	52	76.9
4	14	–	–	–	105	–	–	–	119	88.2
5	–	3	–	7	–	18	–	–	28	64.3
6	–	–	–	–	–	–	9	–	9	100.0
7	1	–	–	–	–	–	–	17	18	94.4
Column total	153	100	74	50	120	21	10	19	547	
Producer Acu%	87.6	83.0	85.1	80.0	87.5	85.7	90.0	89.5		
Overall Acu%	85.6									
Kappa%	82.9									
Referenced 2003										
Classified 2003										
0	136	–	–	–	7	–	2	1	146	93.2
1	1	73	4	4	1	2	–	–	85	85.9
2	5	–	44	–	6	1	–	–	56	78.6
3	1	10	2	29	–	–	–	–	42	69.0
4	11	–	1	–	95	–	–	3	110	86.4
5	–	4	–	2	–	21	–	–	27	77.8
6	–	–	–	–	–	–	15	–	15	100.0
7	2	–	–	–	–	–	–	22	24	91.7
Column total	156	87	51	35	109	24	17	26	505	
Producer Acu%	87.2	83.9	86.3	82.9	87.2	87.5	88.2	84.6		
Overall Acu%	86									
Kappa%	83									
Referenced 2016										
Classified 2016										
0	154	2	1	–	7	–	–	–	164	93.9
1	2	80	2	3	–	3	–	–	90	88.9
2	3	2	69	–	5	–	–	–	79	87.3
3	–	3	–	35	–	2	–	–	40	87.5
4	9	1	3	–	89	–	1	1	104	85.6
5	–	1	–	1	–	33	–	–	35	94.3
6	1	–	–	–	–	–	18	–	19	94.7
7	1	–	–	–	2	–	–	19	22	86.4
Column total	170	89	75	39	103	38	19	20	553	
Producer Acu%	90.6	89.9	92.0	89.7	86.4	86.8	94.7	95.0		
Overall Acu%	89.8									
Kappa%	87.4									

0, intensively cultivated; 1, shrubland; 2, grassland; 3, mixed forest; 4, moderately cultivated; 5, plantation; 6, urban; 7, waterbody; *Producer Acu*, producer accuracy; *User Acu*, user accuracy; *Overall Acu*, overall accuracy

(binary logistic regression) of probability in the Statistical Package for the Social Sciences (SPSS) was used to select the relevant change factors from a list

of expected driving factors in the study. The Dyna-CLUE model utilizes the suitability of sites acquired from the logit model, the conversion elasticity, and

Table 3 Driving factors of change, beta coefficients, and the ROC values of the logistic regression results

	Intensively cultivated	Shrubland	Grassland	Mixed forest	Moderately cultivated	Plantation	Urban
Population density	-0.00326	0.00128	0.00687	0.00711	-0.00072	0.03187	0.00175
Distance to roads	0.00000	-0.00001	0.00008	-0.00036	-0.00007	-0.00048	-0.00473
Distance to towns	0.00010	-0.00006	-0.00011	-0.00004	-0.00002	-0.00024	-
Distance to church	0.00007	-0.00011	-0.00001	-0.00060	-0.00008	-0.00016	-0.00038
Distance waterbody	-0.00004	-	0.00002	0.00011	0.00008	0.00028	0.00032
Elevation	-0.00071	0.00094	-0.00011	0.00207	-0.00009	0.00296	0.00169
Slope	-0.02219	0.05534	-0.03606	0.07737	-0.01575	0.05692	-0.08078
Aspect	0.00131	0.00017	-0.00150	0.00132	-0.00192	0.00083	-
Soil depth	0.00014	-0.00003	-0.00019	-0.00065	-0.00008	-0.00029	-
Soil texture	0.43282	-	0.02185	-	-	-	-
Rainfall	0.00133	-	-0.00279	-0.00149	-0.00138	-0.01732	-
Temperature	-0.14509	0.01043	0.04676	0.52327	0.15055	-1.26177	-
Constant	-0.11747	-4.52056	0.41807	-17.7112	-1.66313	3.93219	-6.95837
ROC value	0.75	0.73	0.71	0.89	0.706	0.94	0.95

the competitive strength of the land-use types to determine the overall likelihood of a change for each grid cell in each land-use type (Verburg & Overmars, 2009). Probability maps of land-use types were produced using a binary logit regression model (Eq. 5).

$$\log\left(\frac{P_i}{1-P_i}\right) = \beta_0 + \beta_1 X_{1,i} + \beta_2 X_{2,i} \dots + \beta_n X_{n,i} \quad (5)$$

where, the probability of a pixel to the presence of a land-use type at location i is represented with P_i and $X_{1,i} - X_{n,i}$ are drivers of change. The coefficient of each land-use driver in the logit model is represented by $\beta_0, \beta_1 - \beta_n$. Using the land use pattern as a dependent variable, the coefficients (β) are calculated in the logit model (Verburg, 2010).

Accuracy of the driving factors and model validation

The validity of the relationship between the land use types and drivers of change was tested using the receiver operating characteristics (ROC) statistics (Verburg & Veldkamp, 2004) in logistic regression. The fitness of the logistic regression in selecting the best driving factor for a land-use change was evaluated with the ROC method. If the ROC value approaches one, the model prediction is perfect, and if it approaches 0.5, it is random (Pontius & Schneider, 2001). The ROC values that are greater

than 0.70 show the regression results are acceptable for predictions (Erdoğan et al., 2011; Mandrekar, 2010). In this study, binary logistic regression analyses were performed with the statistical software SPSS using the stepwise regression method by setting the regression confidence degree to 95% ($\alpha=0.05$). The beta coefficients which did not satisfy the specified confidence degree were excluded from the analysis.

Validation of the Dyna-CLUE model was performed by comparing the maps of predicted land use with the classified ones in the same period of 2016 for the present study. The classified land use map was validated against the Dyna-CLUE model simulated map using the Kappa statistic (Arsanjani et al., 2013). The purpose of this statistical validation was to find out how well the 2016 classified map agreed with the 2016 simulated map in terms of both the quantity and location of cells in each category of land use. The location and quantity agreements in the statistical validation were addressed through the use of the Map Comparison Kit (MCK 3 software) (Hewitt & Escobar, 2011; Visser & De Nijs, 2006) using the Kappa simulation algorithm. In this study, the location similarities between the simulated and the classified maps were measured using Kappa location or “KLc” (Pontius, 2000) whereas the number of cells per category of land uses was quantified using the Kappa “histo” or “KHisto” (Hagen, 2003) (Table 4).

Climate change data (GCM/RCM) under SRES and RCP scenarios

Global Circulation Models (GCMs) are currently being utilized to increase scientific knowledge and understanding of the inconsistency and change of climate variables. In this study, the future climate prediction was made using GCM-RCMs of the IPCC Fourth Assessment Report (IPCC, 2007) emission scenario and the RCPs of the Fifth Assessment Report (IPCC, 2014). Dynamically downscaled daily temperature and rainfall time series of the Regional Model-European Centre Hamburg Model (REMO-ECHAM5) outputs with a resolution of $0.5^{\circ} \times 0.5^{\circ}$ under SRES A1B climate scenario from Max Planck Institute of Meteorology was used for hydrological impact assessments, as recommended by Hattermann (2011). The RACMO22T-RCM model from the driving model of Hadley Global Environment Model 2-Earth System (HadGEM2-ES) in CORDEX-Africa was used for the RCP predictions. Dynamical downscaled precipitation and temperature data of the RCPs from the CMIP5 project with a resolution of $0.44^{\circ} \times 0.44^{\circ}$ are available in the CORDEX-Africa regional climate model (e.g., Brands et al., 2013; Gbobaniyi et al., 2014; Panitz et al., 2014). The RCMs are available from 1951 to 2005 for historical periods and from 2006 to 2100 for future predictions. The patterns of climate change in this study were evaluated using the future scenario period (2025–2099) and the historical/baseline period (1981–2005). RCP2.6 (low), RCP4.5 (low-medium), and RCP8.5 (high) emission scenarios were utilized for the study since CORDEX-Africa prioritizes these scenarios in climate studies in the region (e.g., Alemseged & Tom, 2015).

Bias correction of climate data

Bias correction on A1B and RCP emission scenarios of daily precipitation and temperature were performed using the delta change method to minimize

the systematic statistical deviation of climate model data from the observed data before using it for future climate change studies. The widely used delta-change method (e.g., Bosshard et al., 2011; Graham et al., 2007; Moore et al., 2008) is based on the idea of using RCM-simulated future anomalies to perturb the observed data. Additive and multiplicative corrections were used for temperature and precipitation respectively as presented in Eqs. (6) and (7).

$$T_{fut,corr,d} = T_{obs,d} + (\bar{T}_{fut,m} - \bar{T}_{ref,m}) \tag{6}$$

$$P_{fut,corr,d} = P_{obs,d} * \left(\frac{\bar{P}_{fut,m}}{\bar{P}_{ref,m}} \right) \tag{7}$$

where $T_{fut, corr, d}$ is the future corrected daily temperature (temperature max. and min.), $T_{obs, d}$ is the observed daily temperature for the base years, $\bar{T}_{fut, m}$ is the monthly mean RCM temperature for the future years, and $\bar{T}_{ref, m}$ is the monthly mean RCM temperature of the base years. $\bar{P}_{fut, corr, d}$ is the future corrected daily rainfall, $\bar{P}_{obs, d}$ is the observed daily rainfall, $\bar{P}_{fut, m}$ is the monthly mean RCM rainfall for future years, and $\bar{P}_{ref, m}$ is the monthly mean RCM rainfall for the base years. The delta change is a reliable method for correcting mean values, although it has limits in terms of correcting standard deviations or changes of variance (Addor et al., 2014; Mendez et al., 2020).

Results

LULC maps and accuracy assessment

The LULC maps were classified from satellite images to prepare the land use demand for land use prediction of the watershed. The main LULC classes of the watershed were intensively cultivated, moderately

Table 4 The per category kappa statistics of the classified versus simulated map of 2016

	Intensively cultivated	Shrub land	Grassland	Mixed forest	Moderately cultivated	Plantation	Urban	Water
Kappa	0.750	0.748	0.709	0.763	0.703	0.815	0.857	1.000
KLoc	0.764	0.755	0.741	0.812	0.754	0.845	0.901	1.000
KHisto	0.982	0.991	0.957	0.941	0.897	0.964	0.951	1.000

cultivated, grasslands, shrublands, mixed forests, plantations, urban lands, and waterbodies. From the land-use trends of 1984, 2003, 2016, and 2049, it could be understood that there has been a large increase in cultivation land and a small and gradual increase in urban and plantation areas. While shrublands and grasslands have been mainly converted into cultivation lands, mixed forests have been converted into shrublands and grasslands. The increases in intensively cultivated and moderately cultivated lands were 16.7%, 5.4%, and 11.0% and 38.8%, 8%, and 19.6%, respectively, between the periods of 1984 and 2003, 2003 and 2016, and 2016 and 2049 (Table 5). On the other hand, there has been a large-scale decrease in shrubland and mixed forests in all time periods. There were 23.1%, 25.4%, and 82.5% and 63.4%, 40.7%, and 100% reductions in shrublands and mixed forests between 1984 and 2003, 2003 and 2016, and 2016 and 2049, respectively. Grassland has shown an increasing trend except in the period between 1984 and 2003. Generally, it can be concluded that there has been a great reduction in vegetation and expansion of cultivation lands, mainly due to the shortage of farmlands because of the increasing population in the area. The LULC maps of 1984, 2003, and 2016 real images are presented in Fig. 2a–c sequentially. The overall accuracy of 1984, 2003, and 2016 real or classified images was 85.6, 86.0, and 89.8, respectively, and the kappa statistics of the above-mentioned maps in their order were 82.9, 83.0, and 87.4 (Table 2). The overall accuracy and the kappa values were above the minimum

level of accuracy for the identification of land cover categories from remote sensor data, which indicated the presence of strong agreement between classified and reference data.

The ROC evaluation of the driving factors and validation of the Dyna-CLUE model

The ROC values of the land-use driving factors specified for this study (Millington et al., 2007; Leroux et al., 2017; Lagrosa et al., 2018; Tizora et al., 2018) are presented in Table 3. A total of fourteen driving factors and eight LULC classes were identified and prepared in an ASCII file format for the identification of the best predictive parameter for each LULC class in the study area using the binary logit regression as indicated in Table 3. The ROC statistics range from 0.706 for moderately cultivated land to 0.95 for urban areas. Waterbody did not show a change in size between periods, hence its ROC value is not calculated. At the 95% confidence levels, the regression coefficients and constants were significant, showing that the logit model is good at predicting the probability of occurrence of land uses in the watershed.

Combining the driving factors, land use demand, conversion elasticity, change matrix, and the base map of 1984, the predicted 2016 and 2049 LULC maps were prepared (Fig. 3b, c). The land-use trends of 1984, 2003, 2016, and 2049 indicated that there has been a large increasing trend in cultivation lands and a small increase in urban and plantations area. Driving factors, beta coefficients,

Table 5 The area size of each categorized LULC in 1984, 2003, 2016, and 2049 (ha)

Year	Intensively cultivated	Shrub land	Grassland	Mixed forest	Moderately cultivated	Plantation	Urban	Water
1984	64,153.17	30,888.99	12,611.34	12,277.26	8974.98	183.69	130.86	103.32
2003	74,893.82	23,762.70	12,100.32	4498.38	12,403.62	1233.27	328.14	103.32
2016	78,946.56	17,728.29	14,102.19	2666.88	13,425.48	1454.31	896.58	103.32
2049	87,622.47	3095.73	18,285.93	0.00000	16,057.89	1831.95	2326.23	103.32
Change in LULCs between 1984 and 2003, 2003 and 2016, and 2016 and 2049 (ha)								
1984–2003	10,740.60	–7126.30	–511.00	–7778.90	3428.60	1049.60	197.30	0.00
2003–2016	4052.70	–6034.40	2001.90	–1831.50	1021.90	221.00	568.40	0.00
2016–2049	8675.90	–14,632.60	4183.70	–2666.90	2632.40	377.60	1429.70	0.00
Change in LULCs between 1984 and 2003, 2003 and 2016, and 2016 and 2049 (%)								
1984–2003	16.70	–23.10	–4.10	–63.40	38.20	571.40	150.80	0.00
2003–2016	5.40	–25.40	16.50	–40.70	8.20	17.90	173.20	0.00
2016–2049	11.0	–82.50	29.70	–100.00	19.60	26.00	159.50	0.00

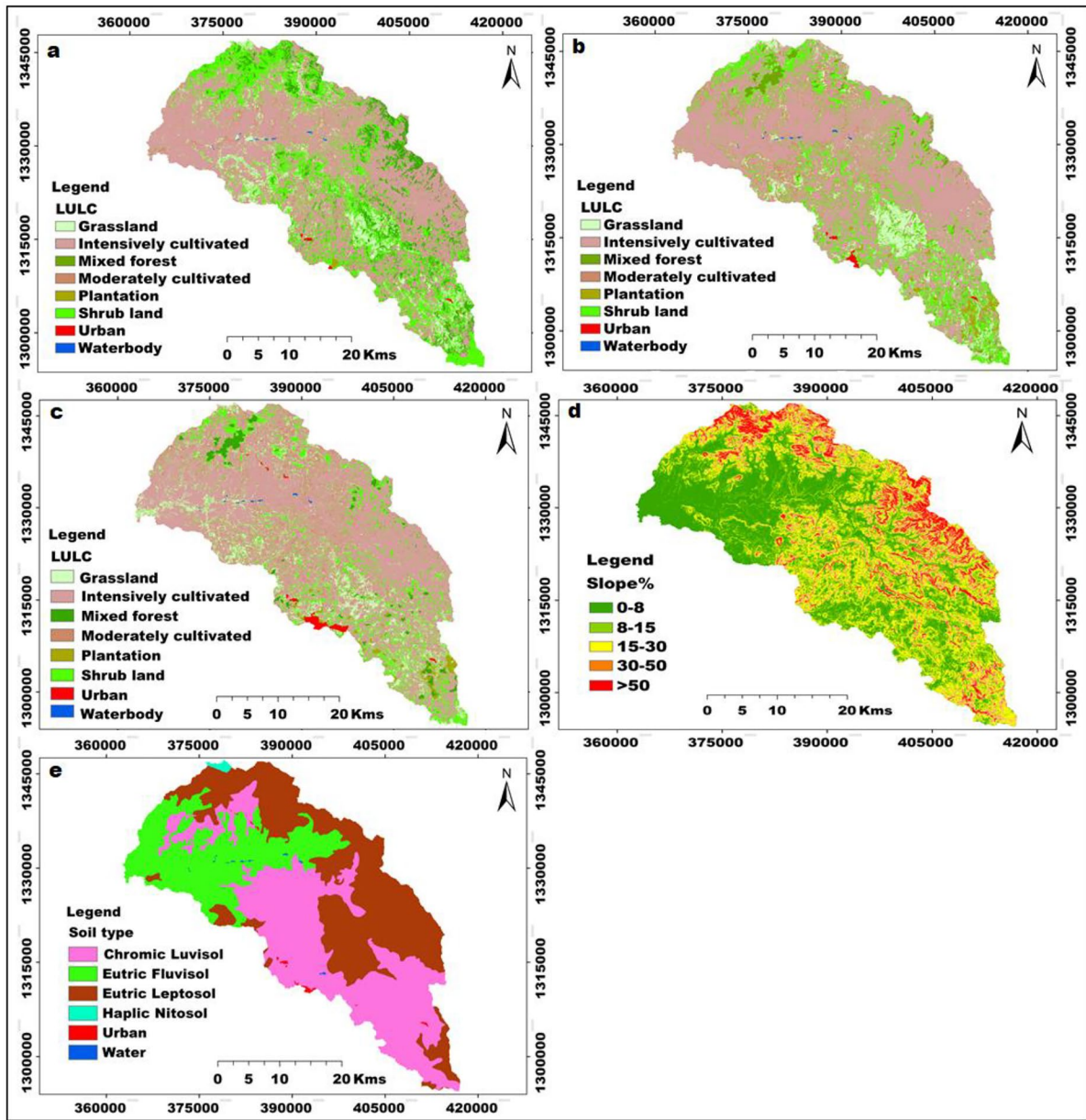


Fig. 2 LULC maps of 1984 (a), 2003 (b), 2016 real or classified (c), slope map (d), and soil map (e)

and ROC values of the logistic regression are presented in Table 3. The increase in intensively cultivated land was 16.7%, 5.4%, and 11.0% between 1984 and 2003, 2003 and 2016, and 2016 and 2049, respectively (Table 5). On the other hand, there were 23.1%, 25.4%, and 82.5% reductions in shrublands between 1984 and 2003, 2003 and 2016, and 2016 and 2049, respectively. The decrease in

mixed forests accounted for 63.4%, 40.7%, and 100% between 1984 and 2003, 2003 and 2016, and 2016 and 2049, respectively. Generally, it can be concluded that there has been a great reduction in vegetation and expansion of cultivation lands in all-time slices. The area size of each LULC in 1984, 2003, 2016, and 2049 and the percentage of change between these periods are presented in Table 5.

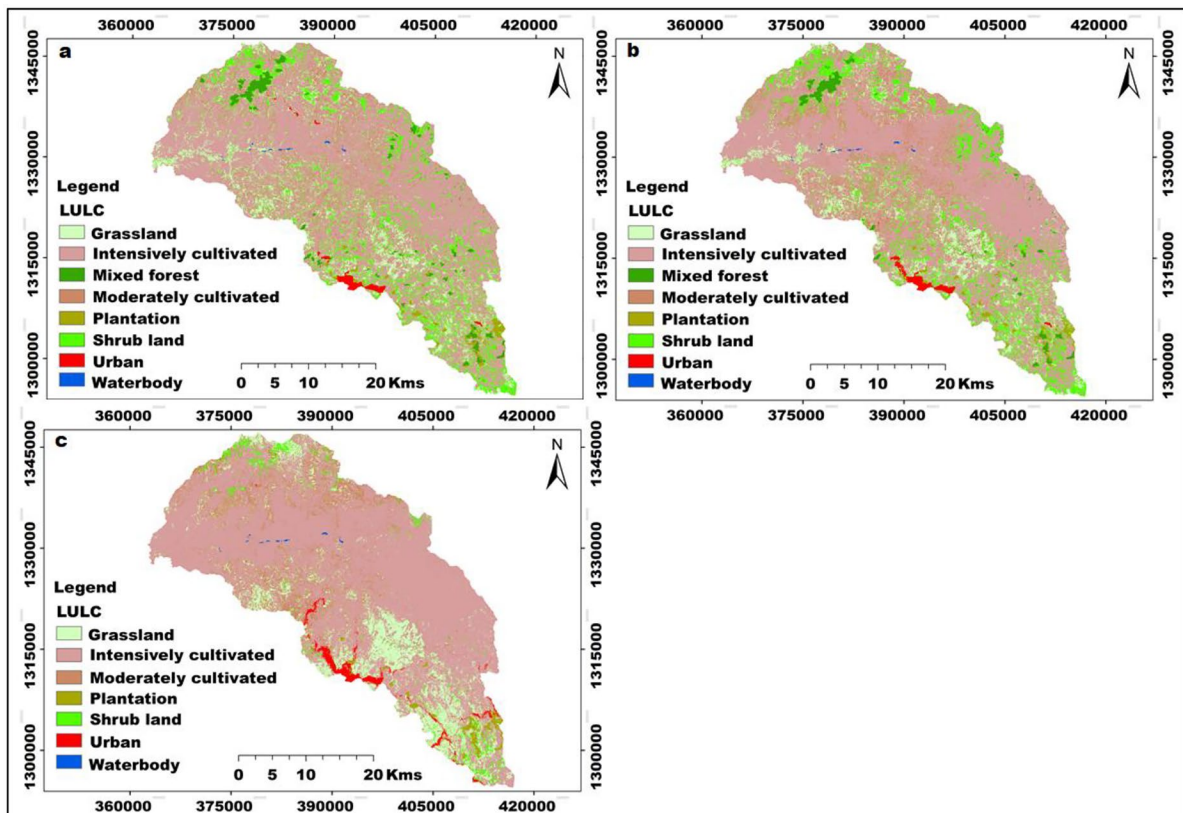


Fig. 3 LULC maps of 2016 real or classified (a), 2016 predicted (b), and 2049 (c)

The model was validated by comparing the predicted land use map with the classified map of the same time period (2016) (Rykiel, 1996; Verburg et al., 2002). The Kappa, “KLocation,” and “KHisto” values of each LULC category are presented in Table 4. The overall Kappa, KLocation, and KHisto values, respectively, were 0.734, 0.762, and 0.963, and the overall accuracy was 0.843. The result of the kappa statistics indicated that the reality and simulated maps have strong agreement; hence, the model is capable of predicting the LULC of the watershed.

Prediction of climate change

Precipitation in A1B and RCP scenarios

The average monthly rainfall of all climate scenarios is presented in Fig. 4. The climate analysis revealed that the high amount of rainfall during July in the

base period is shifted to August in the future scenarios (Fig. 4). The climate predictions showed a general decrease in mean annual precipitation in all-time slices (the 2030s, 2060s, and 2090s) (Table 6). A consistent decrease is shown in seasonal and annual precipitation in all climate scenarios except in the Bega season. In A1B of the Bega season, there might be a high decrease of about 12.7% in the 2030s and an increase of about 16% in the 2060s (Fig. 5). The highest decrease is shown in the 2090s of the Belg season by about 57.7%. In general, the projected precipitation in the watershed has a decreasing trend in all scenarios (Table 6; Fig. 6). The seasonal changes in precipitation in the 2030s, 2060s, and 2090s of all climate scenarios are presented in Fig. 5. RCP2.6, low range, RCP4.5 mid-range, and RCP8.5 high-range climate scenarios with a radiative forcing of 2.6, 4.5, and 8.5 W/m² by 2100, respectively (Riahi et al., 2011; Thomson et al., 2011) were expected to capture reasonable ranges in climatic and hydrological projections.

Fig. 4 Monthly rainfall in all climate periods

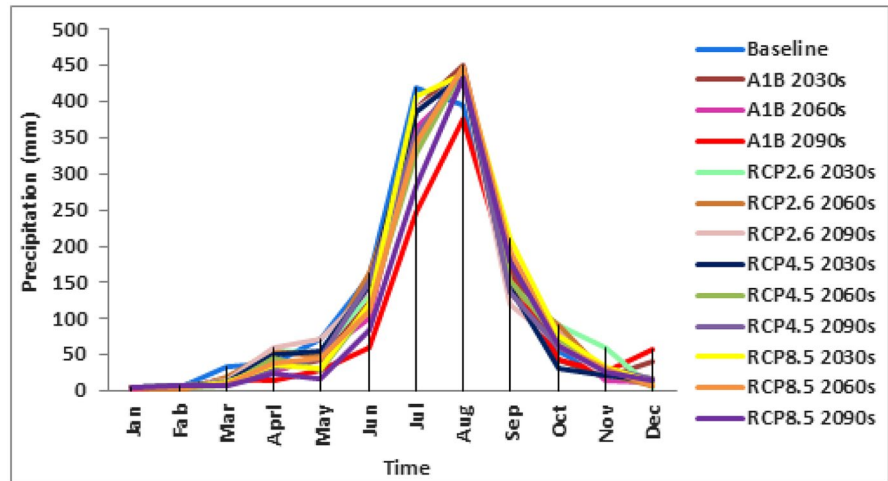


Table 6 Changes (%) in precipitation in all climate scenario periods in the 2030s, 2060s, and 2090s

Climate scenarios	Time slices		
	2030s	2060s	2090s
A1B	-5.1	-6.6	-27.7
RCP2.6	-3.8	-1.9	-2.4
RCP 4.5	-4.9	-8.8	-6.2
RCP 8.5	-0.82	-5.4	-16.7

In RCP2.6, the highest increase is in the Bega by 55.3%, and the lowest decrease in Krimt by 3.78% compared to the base period in the 2060s. The mean annual decrease is about 2.7% (Table 6). In the 2060s

of RCP4.5, the highest decreases in Belg and Kiremt precipitation will be 40.9% and 8.5% sequentially (Fig. 5). The annual precipitation showed a decrease in all RCP4.5 by 4.9%, 8.8%, and 6.2% in the 2030s, 2060s, and 2090s, respectively (Table 6; Fig. 5). In RCP8.5, a continuous increase is shown in the Bega by 37.5%, 18.9%, and 23.6%, and a decrease in Belg by 44.0%, 34.7%, and 65.4% in the 2030s, 2060s, and 2090s, respectively (Fig. 5). Figure 5 illustrates the seasonal and annual change in precipitation in all climate scenarios.

In the 2030s, the annual average precipitation will be expected to decrease by 5.8% in A1B, 3.8% in RCP2.6, 4.9% in RCP4.5, and 0.8 in RCP8.5. In the 2060s (mid-century), precipitation is predicted

Fig. 5 Annual and seasonal change in precipitation in climate scenarios from the baseline period of 1981-2005

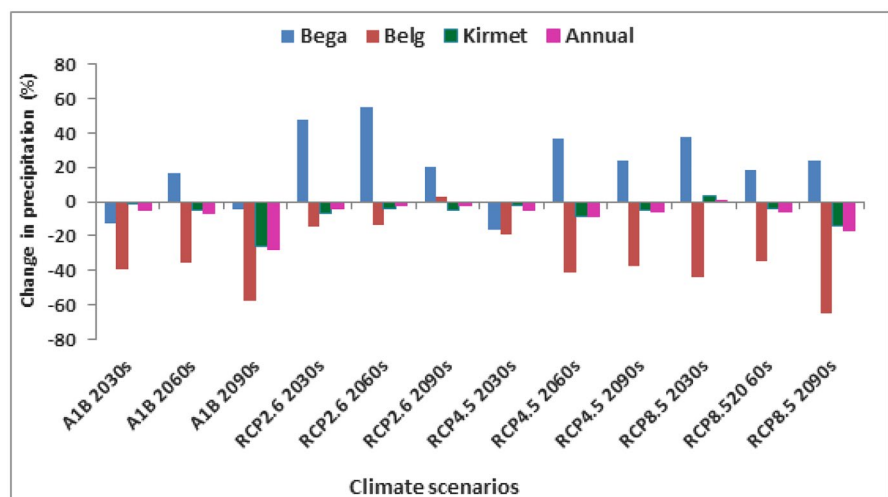
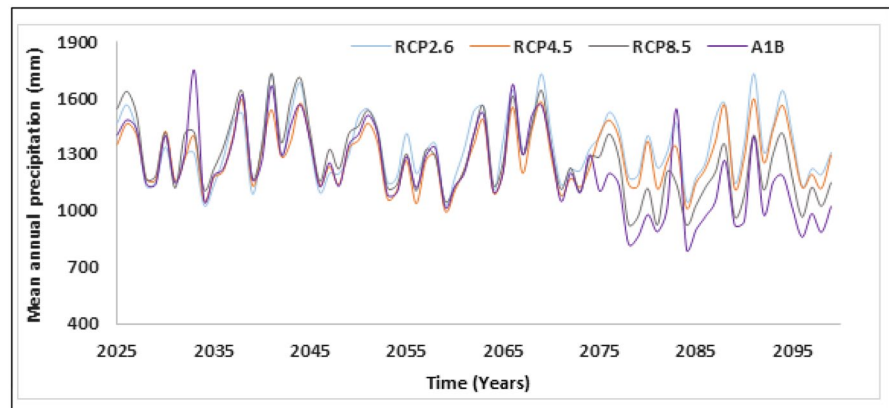


Fig. 6 Future trend of mean annual precipitation in A1B and RCPs



to decrease by 6.6% in A1B, 1.9% in RCP2.6, 8.8% in RCP4.5, and 5.4% in RCP8.5. The 2090s (end-of-century) will show a decline in precipitation by 27.7% in A1B, 2.4% in RCP2.6, 6.2% in RCP4.5, and 16.7% in RCP8.5 in the Rib watershed (Table 6).

Temperature in A1B and RCP scenarios

The projected maximum and minimum temperatures showed an increasing trend in all A1B scenarios compared to the baseline temperature of 1981–2005 (Fig. 9). In all scenarios, a maximum increase is observed in the 2090s. Belg showed the highest increase in both temperatures in all scenarios. Mean monthly change in maximum temperature varies between +0.9 and +1.87 °C in the 2030s, +2.1 and +2.9 °C in 2060s, and +3.4 and +4.65 °C in the 2090s; whereas minimum temperature varies between -0.01 and +2.67 °C in 2030s, +1.1 and +4.0 °C in 2060s, and +2.95 and +4.65 °C in 2090s in A1B scenario compared to the baseline period of 1981–2005 (Fig. 7a, b). A high maximum temperature increase of 1.87 °C, 2.94 °C, and 4.65 °C is expected in May in the 2030s, 2060s, and 2090s, respectively. The Belg season showed the highest increase in maximum temperature by +1.58 to 4.5 °C in 2030 and 2090s, respectively, and minimum temperature increase by +1.94 to +4.36 °C in the same periods. The annual average increase varies between 1.3 °C in the 2030s and 4.16 in 2090s in maximum temperature and +1.3 in the 2030s and +3.8 °C in the 2090s in minimum temperature (Fig. 7).

In RCP2.6, maximum temperature varies between +0.7 and +2.0 °C in the 2030s, +1.0 and +1.87 °C in the 2060s, and +0.75 and +1.8 °C in 2090s from the baseline period of 1981–2005 (Fig. 7a). “Belg” is predicted to show the

highest increase by +1.5 and +2.27 °C in maximum and minimum temperatures respectively in the 2060s. “Kiremt” is predicted to show a lower increase in both temperatures in RCP2.6 scenario (Fig. 7a, b). The annual average increase varies between 1.4 and 1.35 °C in maximum temperature and 1.59 °C and +1.48 °C in minimum temperature in the 2030s and 2090s, respectively (Figs. 7a, b and 8). The change in monthly, seasonal, and annual maximum and minimum temperatures in all scenario periods is illustrated in Fig. 7a, b, respectively.

The Bega and Belg maximum temperature increase in RCP4.5 of the 2030s, 2060s, and 2090s, respectively, will be +1.59 °C, 2.29 °C, and 2.53 °C and +1.7 °C, +2.3 °C, and +2.52 °C. In RCP4.5, Bega and Belg minimum temperature increase in the 2030s, 2060s, and 2090s of RCP4.5 sequentially will be +1.3 °C, +1.7 °C, and +2.0 °C and +1.66 °C, +2.49 °C, and +2.64 °C (Fig. 7a, b). The annual maximum temperature increase varies between +1.59 °C in the 2030s and +2.49 in the 2090s, and the annual minimum temperature increase ranges between +1.5 and +2.35 °C in the 2030s and 2090s, respectively (Fig. 7a, b).

August and June showed a higher increase in maximum temperature in the 2090s of RCP4.5 by 4.5 °C and +4.98 °C. The highest increase is in the Belg season by 4.75 °C and 4.82 °C in maximum and minimum temperatures, respectively, in the 2090s. The annual increase in maximum temperature might be +1.79 °C, +3.55 °C, and +4.7 °C in the 2030s, 20,605, and 2090s respectively. The minimum temperature (greater than +4.5 °C) increases faster than the maximum temperature in all months of the 2090s.

It is expected that the average annual maximum and minimum temperatures might increase by 1.3 °C

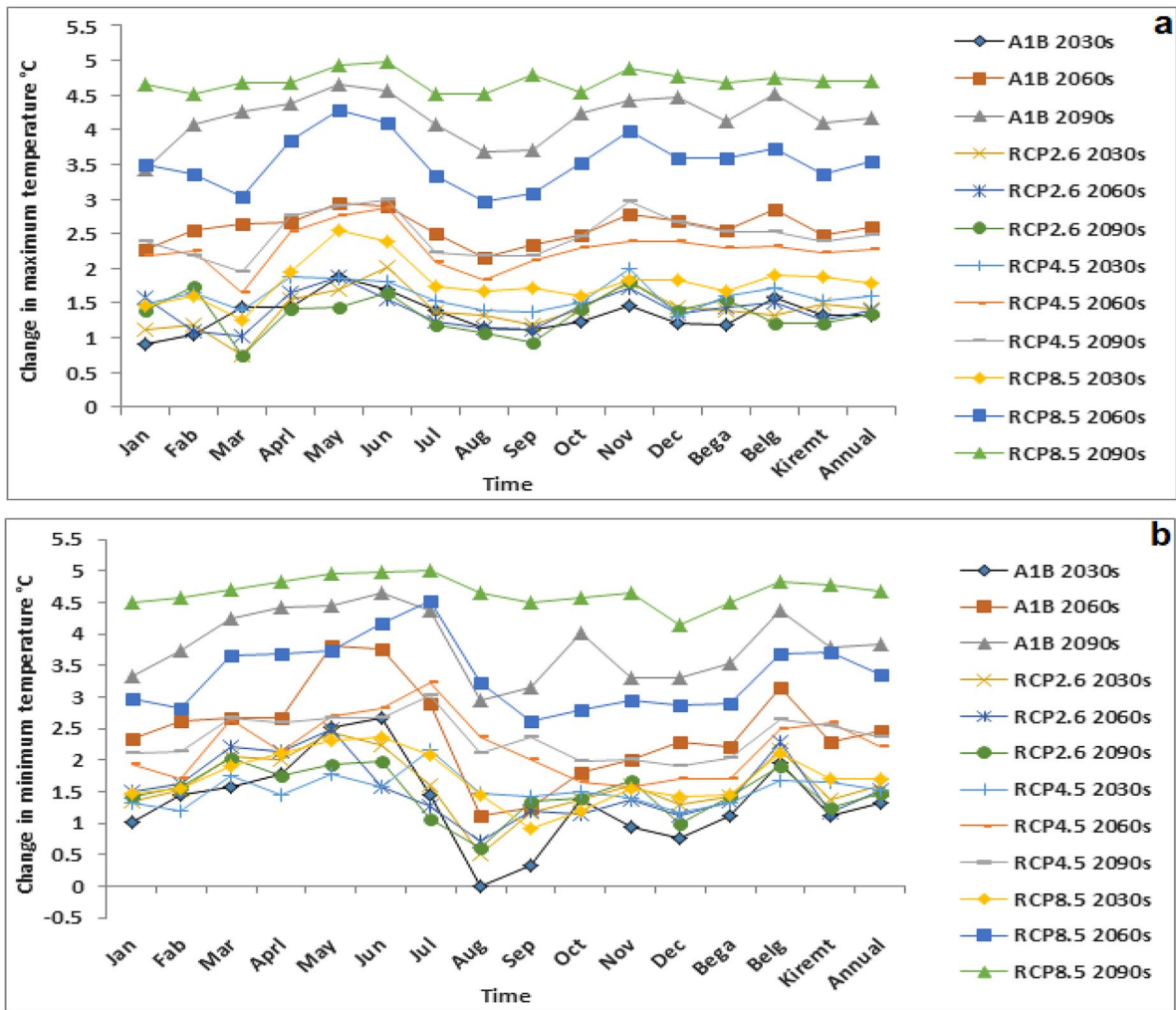


Fig. 7 Change in monthly, seasonal and annual maximum (a) and minimum (b) temperature in A1B and RCPs from the baseline period of 1981–2005

and 1.3 °C in the 2030s, 2.6 °C and 2.5 °C in the 2060s, and 4.1 °C and 3.82 °C in the 2090s, respectively, in the A1B scenario compared to the baseline period of 1981–2005. The average annual increase of maximum and minimum temperatures respectively in the 2030s is 1.4 °C and 1.59 °C in RCP2.6, 1.59 °C and 1.52 °C in RCP4.5, and 1.79 °C and 1.69 °C in RCP8.5 (Fig. 7a, b). In the 2060s, the maximum and minimum temperature increases will be 1.39 °C and 1.5 °C in RCP2.6, 2.28 °C and 2.2 °C in RCP4.5, and 3.55 °C and 3.38 °C in RCP8.5, and in the 2090s, they will be 1.35 °C and 1.48 °C in RCP2.6, 2.49 °C and 2.35 °C in RCP4.5, and 4.7 °C and 4.67 °C in RCP8.5. The result showed

that in RCP2.6, the increase in minimum temperature exceeds the maximum temperature and that in RCP4.5 and RCP8.5, the increase in maximum temperature is higher than the minimum temperature. The comparison between the 2030s, 2060s, and 2090s in maximum and minimum temperatures in all climate scenarios is presented in Fig. 8. The trend of an increase in mean annual maximum and minimum temperatures in all climate scenarios is presented in Fig. 9. In terms of the analysis of this study, a high decrease in precipitation and an increase in temperature are observed, especially in the 2090s of A1B and RCP8.5. The 2090s’ mean maximum temperature increase of up to 1.8 °C in RCP2.6, 2.98 °C in

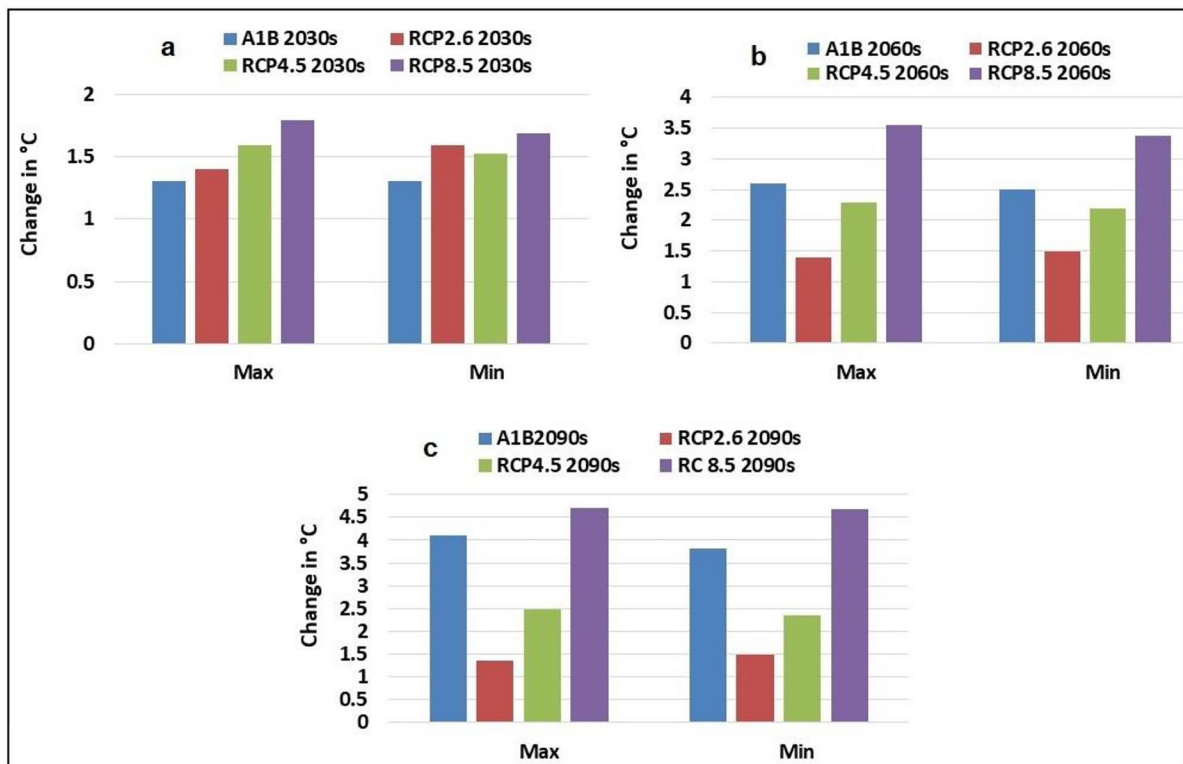


Fig. 8 Change in maximum and minimum temperatures in the 2030s (a), 2060s (b), and 2090s (c) in A1B and RCPs from the baseline period of 1981-2005

RCP4.5, 4.93 °C in RCP8.5, and 4.65 °C in A1B of this study, as well as the mean minimum temperature increase of up to 2.0 °C in RCP2.6, 3.0 °C in RCP4.5, 4.99 °C in RCP8.5, and 4.65 °C in A1B, is comparable to the 2090s' projected maximum limit of the IPCC (2014), which is reported as 1.7 °C under RCP2.6, 2.6 °C under RCP4.5, and 4.8 °C under RCP8.5.

Sensitivity analysis, calibration, validation, and performance evaluation of SWAT model

Sensitive parameters that have a strong influence on model outputs were identified using monthly observed streamflow and sediment data. Thirteen parameters for flow and eight parameters for sediment were identified as the most sensitive parameters for calibration using the global sensitivity analysis procedure. The sensitive parameters for both flow and sediment with their rankings are presented in

Table 7. To increase the fit between the observations and simulations, they selected calibrated parameters to undergo further simulations, and based on *t*-stat and *p*-value, the ranks were determined from the last iteration of SUFI-2. As the absolute value of the *t*-stat increases and the *p*-value decreases, the parameter sensitivity becomes higher (Abbaspour et al., 2015). The top five sensitive parameters of flow were initial SCS CNII (CN2), the soil layer available water capacity (SOL_AWC), maximum canopy storage (CANMX), deep aquifer percolation fraction (RCHRG_DP), and Manning's *n* value for overland flow (OV_N) (Table 7). For sediment yield, the three higher sensitive parameters were channel erodibility factor (CH_ERODMO), exponent of re-entrainment parameter for channel sediment routing (SPEXP), and minimum value of the USLE C-factor applicable to the land cover (USLE_C) (Table 7). Table 7 presents sensitive parameters and their ranks of flow and sediment.

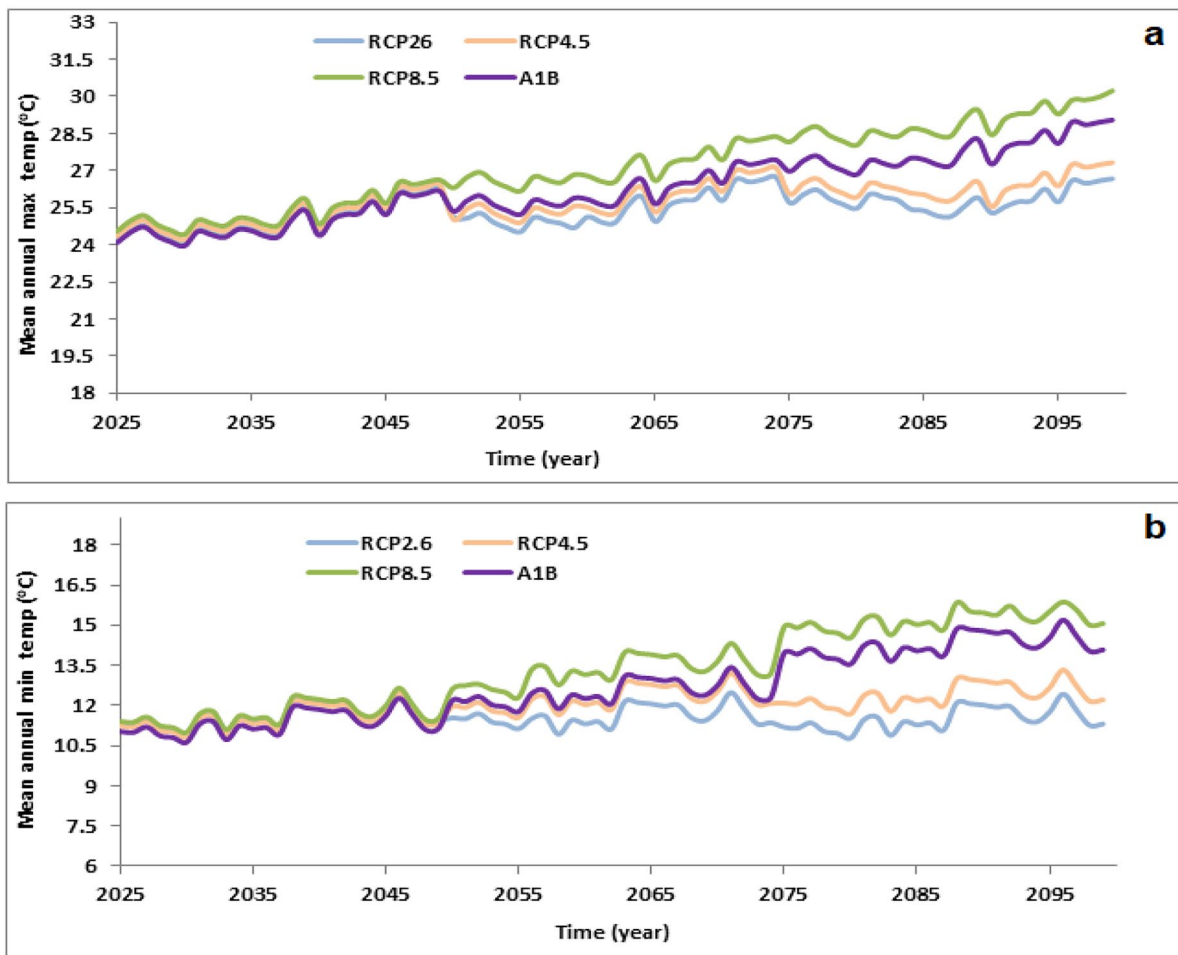


Fig. 9 Future trend of mean annual maximum (a) and minimum (b) temperature in A1B and RCPs

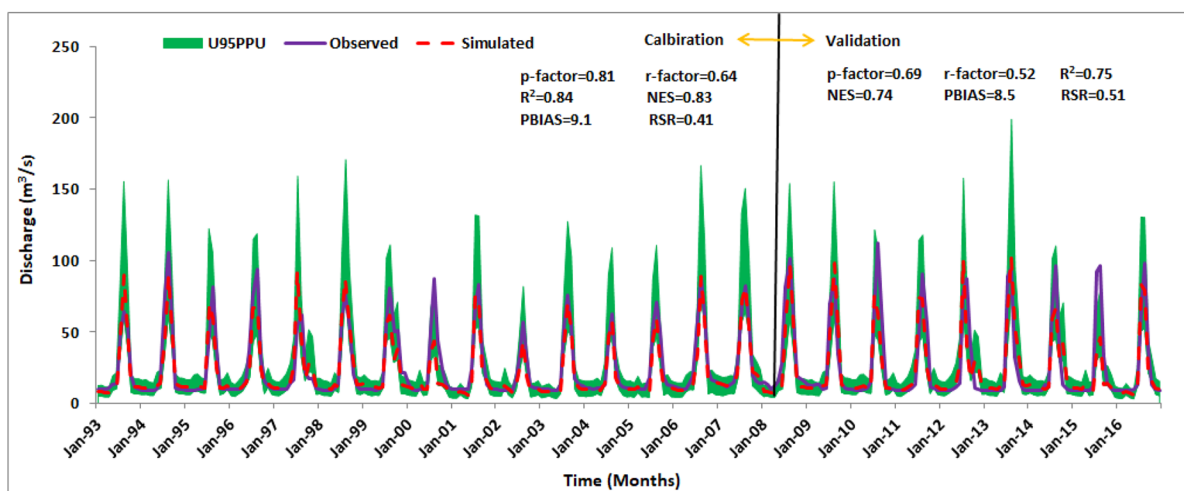
Using the sensitive parameters selected by the sensitivity analysis, model calibration and validation of flow and sediment were performed in the periods of 1993–2007 and 2008–2016, respectively, with a warm-up period from 1990 to 1993. The monthly flow simulation characterizes the observed values in the calibration period with the statistical values of R^2 , NSE, PBIAS, and RSR of 0.84, 0.83, 9.1, and 4.1, respectively (Fig. 10). Flow validation indicated in the statistics of R^2 , NSE, PBIAS, and RSR is 0.75, 0.82, 8.5, and 5.1, respectively (Fig. 10). The capability of SWAT in capturing flow and sediment could be observed from the time series of the monthly calibration versus validation diagram illustrated in Figs. 10 and 11, respectively. After an adequate threshold of

flow calibration was attained, calibration of sediment yield was conducted. The statistics of monthly simulated sediment in calibration characterize observations by R^2 , NSE, PBIAS, and RSR values of 0.74, 0.72, 18.8, and 0.53, respectively (Fig. 11). With the same parameters of the calibrations, the statistical values of sediment yield validation were represented by R^2 , NSE, PBIAS, and RSR, with values of 0.61, 0.60, 18.7%, and 0.64, respectively (Fig. 11). The results of calibration and validation of flow and sediment revealed that the simulations are within adequate range compared to observations. P-factor and R-factor of flow in calibration and validation, respectively were (0.81, 0.69) and (0.64, 0.52) (Fig. 10), and of sediment yield in the same order above were (0.62, 0.47) and

Table 7 Parameters, optimized values, and ranks of flow and sediment calibration

Parameters	Description	SWAT default range	Fitted value	Rank
Flow parameters				
r_CN2	Initial SCS CNII	±0.2	−0.11	1
r_SOL_AWC	Soil available water capacity	0–1	0.77	2
r_CANMX	Maximum canopy storage	0–100	94.4	3
r_OV_N	Manning’s “n” value for overland flow	0.01–30	22.6	5
v_SURLAG	Surface runoff lag time	0.05–24	23.7	7
v_RCHRG_DP	Deep aquifer percolation fraction	0–1	0.42	4
v_GWQMN	Threshold water depth in the shallow aquifer for flow (mm)	0–5000	4922	8
v_ESCO	Soil evaporation compensation factor	0–1	0.02	9
r_SOL_K	Saturated hydraulic conductivity	0–2000	17.6	6
r_HRU_SLP	Average slope steepness	0–1	0.76	10
v_GW_DELAY	Groundwater delay (days)	0–500	337	11
v_ALPHA_BF	Base flow alpha factor or base flow recession constant (days)	0–1	0.12	12
v_REVAPMN	Threshold depth of water in shallow aquifer for “revap” (mm)	0–500	49.2	13
r_SLSUBBSN	Average slope length	10–150	31	14
Sediment parameters				
v_CH_ERODMO	Channel erodibility factor	0–1	0.95	1
v_SPEXP	Exponent of re-entrainment parameter for channel sediment routing	1–1.5	1.48	2
v_SPCON	Linear re-entrained factor parameter for channel sediment routing	0.0001–0.01	0.0038	4
v_CH_COV2	Channel cover factor	−0.001–1	1.0	8
r_USLE_C	Min value of USLE C-factor applicable to the land cover	0.001–0.5	0.47	3
v_USLE_P	USLE support parameter	0–1	0.42	5
r_HRU_SLP	Average slope steepness	0–1	0.48	6
r_SOL_AWC	Available water capacity of the soil layer	0–1	0.36	7

In the parameters, v__ refers to the existing value of the parameter, which is to be substituted by the given value, and r__ refers to the existing value of the parameter, which is multiplied by (1 + the given value) (Abbaspour et al., 2015)

**Fig. 10** Monthly flow calibration (1993–2007) and validation (2008–2016) for Rib watershed

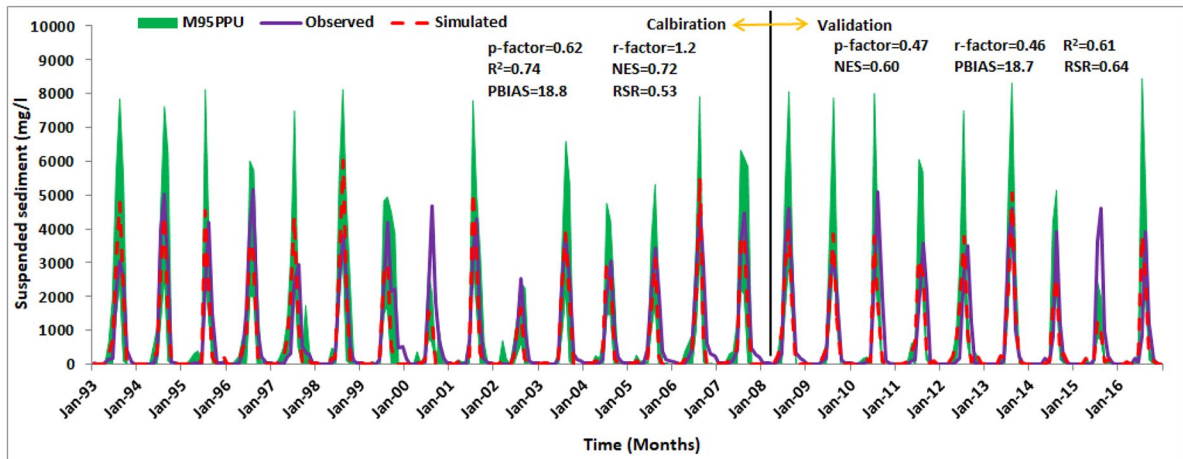


Fig. 11 Monthly sediment calibration (1993–2007) and validation (2008–2016) for Rib watershed

(1.2, 0.46) (Fig. 11). Flow has a better P-factor than the R-factor (thickness of the 95PPU) value both in calibration and validation (Fig. 10) whereas sediment has a better R-factor than the P-factor, particularly during the validation (Fig. 11). In general, from the calibration and validation values, it can be concluded that the goodness of fit statistics reveal that the observed and simulated average monthly flow and sediment are in good agreement. The fit between observed and simulated values of flow and sediment is represented in Figs. 10 and 11, respectively.

Hydrological components and sediment yield response to LULC and climate changes

The LULC maps of 2016 (base map), 2049 (predicted map), and predicted climate from 2025 to 2099 were used to show their impact on the hydrology and sediment of the watershed. The effect of a combination of FLULCC&FCC and FCC was investigated. On a yearly and monthly basis, the hydrological components of surface runoff, lateral flow, groundwater flow, total water yield (WYLD), evapotranspiration (ET), and sediment yield were examined.

Impacts of FCC on hydrological components and sediment yield

In general, surface runoff showed a consistent decrease in A1B scenario simulations on both FCC and FLULCC&FCC scenarios compared with the

base period. The decrease of surface runoff in A1B of the FCC scenario in the time slices of the 2030s and 2090s was between 10.2 and 42.7%, respectively (Table 8; Fig. 12a, c). Except for the 2060s of RCP2.6, it showed an increasing trend in all RCPs. It varies between -4.1 in the 2060s of RCP2.6 and 23.5% in the 2030s of RCP8.5. It might also show a lower increase in the 2030s of RCP2.6 by 0.1% in the FCC scenario. The highest increase of 23.5% is predicted in the 2030s of RCP8.5 (Table 8; Fig. 12a).

Lateral flow and groundwater flow show a decreasing trend in all SRES A1B and RCP time slices. The highest decrease is predicted in the A1B than the RCPs. Lateral flow shows a decrease of 9.2% and 31% in A1B of the 2030s and 2090s sequentially whereas groundwater flow decreased by 20.6% and 52.5% in the same order in the above time periods (Table 8; Fig. 12a, c). The change in lateral flow varies between -7 and 3.5% in the 2090s and 2030s respectively in RCP8.5. This means that the highest increase and decrease are expected to occur in RCP8.5. The highest and lowest decrease in groundwater flow is predicted in RCP8.5 by 23.5% and 6.7% in the 2090s and 2030s sequentially (Table 8). While Table 8 shows the percentage change of hydrologic components due to the climate change scenario, Fig. 12a-c depicts these changes in the 2030s, 2060s, and 2090s bands.

WYLD shows a decreasing trend in all SRES A1B and RCP time slices except in the 2030s of RCP8.5. The highest amount of decrease in WYLD

Table 8 Percentage (%) change of annual average hydrologic components in the FCC scenario

Scenario	Surface runoff	Lateral flow	Groundwater	Total WYLD	ET	Sediment
SRES A1B						
2030s	-10.2	-9.2	-20.6	-15.9	9.2	-45.8
2060s	-18.4	-11.8	-24.5	-21.3	10.2	-50.0
2090s	-42.7	-31.0	-52.5	-47.3	7.0	-19.9
RCP2.6						
2030s	0.1	-2.7	-14.3	-8.1	16.4	-17.6
2060s	-4.1	-3.0	-14.0	-9.5	15.7	-31.0
2090s	7.8	2.0	-8.3	-1.6	19.0	-21.3
RCP4.5						
2030s	9.5	-0.2	-11.9	-3.1	18.7	15.3
2060s	2.6	-4.8	-19.0	-9.9	16.9	-15.7
2090s	10.7	1.1	-11.4	-2.3	19.2	-9.3
RCP8.5						
2030s	23.5	3.5	-6.7	5.3	15.8	25.9
2060s	2.7	-3.5	-17.5	-9.0	18.5	-7.9
2090s	11.1	-7.0	-23.5	-9.4	16.2	64.0

is predicted during the A1B periods. The decreasing values in the A1B of the 2030s and 2090s range between 15.9 and 47.3%, respectively. The change in total WYLD ranges between -9.9 in the 2060s of RCP4.5 and 5.3% in the 2030s of RCP8.5. It shows an increase only in the 2030s of RCP8.5 by 5.3% compared to the base period (Table 8). Evapotranspiration (ET) shows an increase in all A1B and RCP periods. A higher increase is observed in the RCPs than in the A1B prediction. The increasing trend of ET varies between 7 in the 2090s and 10.2% in the 2060s time slices of the A1B climate model. Its increase varies between 15.7 in the 2060s of RCP2.6 and 19.2% in the 2090s of RCP4.5.

In general, sediment yield is expected to show a decrease in both FLULCC&FCC and FCC scenarios. In the FCC scenario higher decrease in sediment yield is observed in A1B than in the RCPs (Table 8). The range of decrease of sediment yield is between 19.9 and 50% in the 2090s and 2060s of A1B. It shows increasing and decreasing fluctuations in the RCPs. It might show an increase in the 2030s of RCP4.5 and 2030s and 2090s of RCP8.5 by 15.3%, 25.9%, and 64%, respectively. In the other RCP scenarios, it shows a decrease in value. The highest increase is expected in RCP8.5. The range of variation in sediment yield in the RCPs is between -31 in the 2060s of RCP2.6 and 64% in the 2090s of RCP8.5. The change in water balance components and sediment

yield in the 2030s, 2060s, and 2090s of A1B and RCPs in the FCC scenario is presented in Table 8 and Fig. 12a-c.

Impacts of FLULCC&FCC on hydrological components and sediment yield

There is a decrease in surface runoff in A1B and an increase in RCP climate predictions. Its decreasing values in A1B for the 2030s and 2090s are between 5.6 and 39.6%, respectively. It might show an increasing trend with a range between 0.3 and 28.7% in the RCPs compared with the baseline. A lower increase in surface runoff might be observed in the 2060s of RCP2.6, RCP4.5, and RCP8.5 by 0.3%, 7.2%, and 7.3%, respectively. The highest increase of 28.7% is predicted in the 2030s of RCP8.5 (Table 9; Fig. 13a). The 2090s of RCP2.6, RCP4.5, and RCP8.5 will show a significant increase in the surface runoff by 12.5%, 15.5%, and 15.5%, respectively (Fig. 13c). The results showed that higher surface runoff is observed in the FLULCC&FCC scenario than in the FCC scenario simulations (Fig. 13). This indicated that LULC change has a significant impact on the hydrologic response of the watershed.

Lateral flow and groundwater flow show a decrease in all A1B and RCPs, with the highest decrease in the A1B prediction. In the 2030s and 2090s of A1B, the range of decrease in lateral flow is between 16.% and

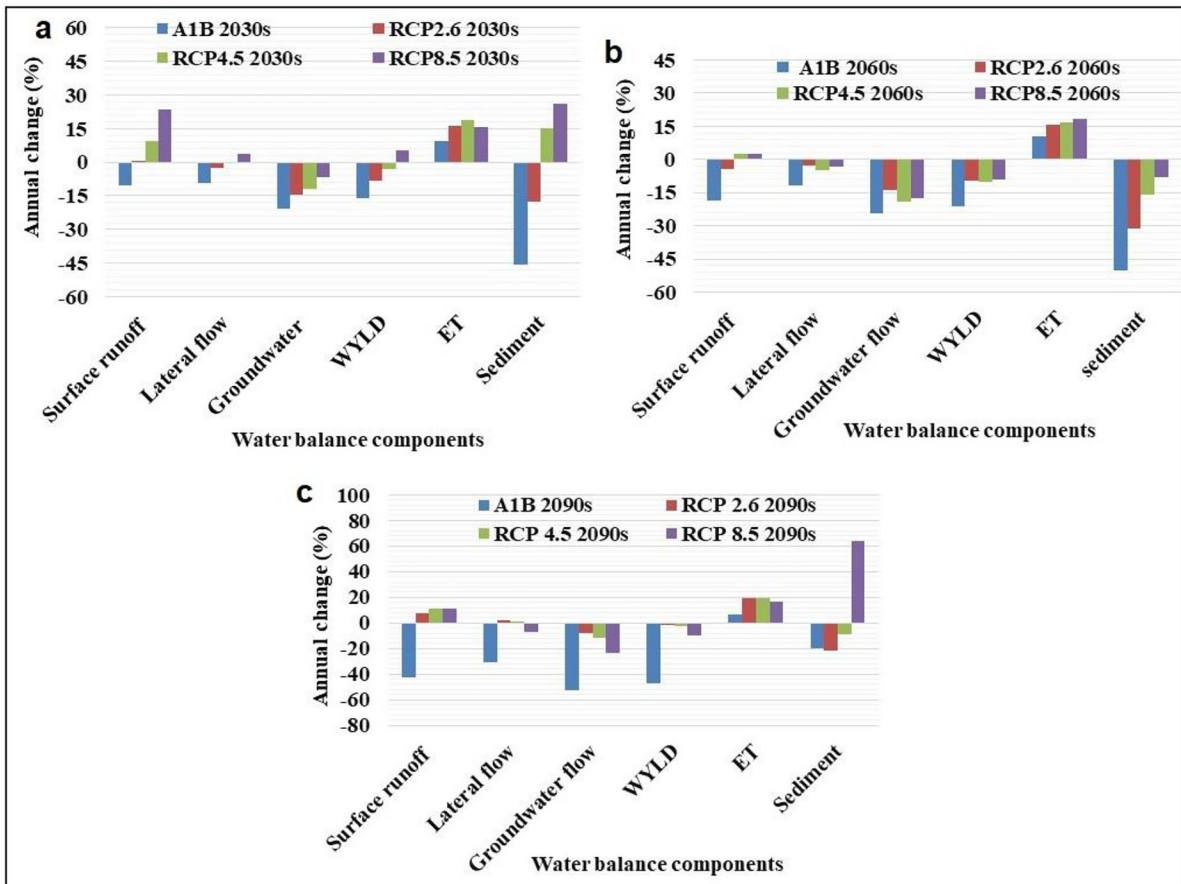


Fig. 12 Percentage (%) change of annual average hydrologic components in FCC scenario (the 2030s (a), 2060s (b), 2090s (c)) in A1B and RCPs

35.4%, and groundwater is between 21.9 and 53.3%, respectively (Table 9; Fig. 13a, c). There might be a decrease in lateral flow and groundwater flow with a range between 3.7 and 13.6% and 7.1 and 22.4% in the 2030s and the 2090s, respectively, in RCP8.5. So the highest and lowest decrease is shown in RCP8.5.

Total water yield shows a decreasing trend in the A1B and RCPs, with the highest decrease in the A1B prediction. Its decrease in the 2030s and 2090s of A1B ranges between 15.6 and 46.9%, respectively. The change ranges between -9.5 in the 2060s of RCP4.5 and 5.6% in the 2030s of RCP8.5. It shows an increase only in the 2030s of RCP8.5 by 5.6%, but in the other scenarios, it shows a decreasing trend. An increase in ET is shown in all A1B and RCP periods with a higher increase in the RCPs. The range of increase is between 6.5 in the 2090s and 9.7% in the

2060s of A1B. Its increase varies between 15.2 in the 2030s of RCP8.5 and 18.7% in the 2090s of RCP4.5. As it is shown in Table 9, there is a comparable increase in ET in all RCP periods.

Sediment yield shows a decrease in all A1B time slices due to the highest decrease in precipitation than the RCPs. On average, the decrease in precipitation is 13.1% in the A1B and 5.6% in the RCPs (Table 9), and this higher decrease in precipitation contributed to a lower sediment yield loss in the A1B periods even though the decline of vegetation is observed in the watershed. The range of decrease in sediment yield in the 2090s and 2060s of A1B is between 1.9 and 35.2, respectively. It shows a decline of 1.9% and 13% only in the 2060s and 2090s of RCP2.6 and an increase in all other RCPs. The highest increase in sediment yield is 82% in the 2090s of RCP8.5

Table 9 Percentage (%) change of average annual hydrologic components in the FLULCC&FCC scenarios combined

Scenario	Surface runoff	Lateral flow	Groundwater	Total WYLD	ET	Sediment
SRES A1B						
2030s	-5.6	-16.7	-21.9	-15.6	8.7	-29.6
2060s	-14.4	-17.4	-25.7	-20.9	9.7	-35.2
2090s	-39.6	-35.4	-53.3	-46.9	6.5	-1.9
RCP2.6						
2030s	4.6	-9.2	-15.9	-7.8	15.9	3.2
2060s	0.3	-9.2	-15.5	-9.1	15.2	-13.0
2090s	12.5	-4.6	-10.1	-1.3	18.6	-1.9
RCP4.5						
2030s	14.2	-6.9	-13.6	-2.8	18.3	39.8
2060s	7.2	-11.3	-20.6	-9.5	16.3	6.0
2090s	15.5	-5.8	-13.2	-2.0	18.7	14.4
RCP8.5						
2030s	28.7	-3.7	-7.1	5.6	15.3	54.6
2060s	7.3	-9.9	-19.2	-8.6	18.0	15.3
2090s	15.5	-13.6	-22.4	-9.4	16.1	82.0

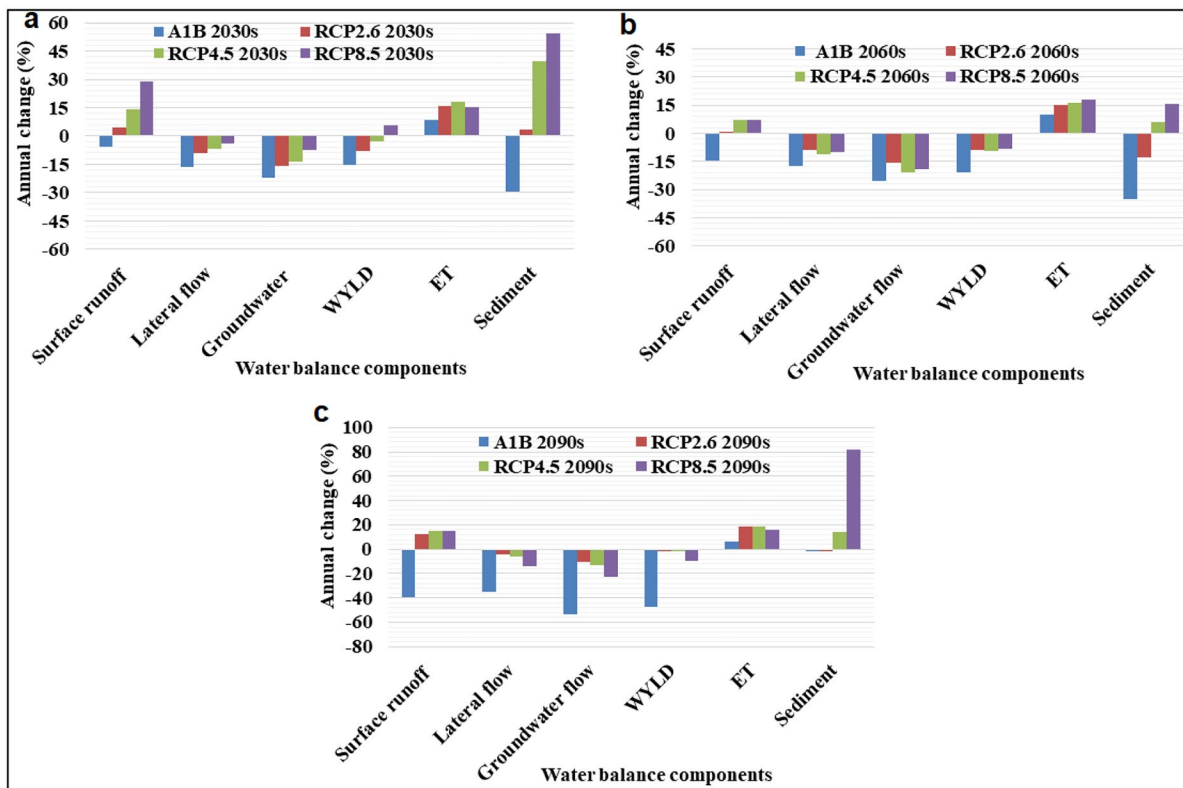


Fig. 13 Percentage (%) change of annual average hydrologic components in FLULCC&FCC scenario (the 2030s (a), 2060s (b), 2090s (c)) in A1B and RCPs

and the highest decrease is -13% in the 2060s of RCP2.6 (Table 9). The annual percentage change of hydrologic components and sediment yield in the 2030s, 2060s, and 2090s in the A1B and RCPs in the FLULCC&FCC scenario is presented in Fig. 13a–c.

Lateral flow shows a higher decrease in the FLULCC&FCC scenario than the FCC scenario whereas groundwater flow will show almost the same amount of reduction in both scenarios (Fig. 13). The range of variation in total WYLD is almost the same in the two scenarios. In general, a higher increase in sediment yield is projected in the FLULCC&FCC scenario than in the FCC scenario. This might be attributed to the increasing conversion of LULC, mainly the expansion of cultivated lands at the expense of vegetation. As Table 9 illustrates the change in water balance components in all climate periods, Fig. 13a–c depicts these changes in the 2030s, 2060s, and 2090s bands due to FLULCC&FCC in combination.

Discussion

Prediction of precipitation

Rainfall predictions are much more unreliable than temperature predictions, having larger spatial and seasonal inconsistencies (Orlowsky & Seneviratne, 2012). Similarly, the IPCC (2014) reported that future rainfall predictions will not show uniform patterns. A change in precipitation was between -12.7 and $+16\%$ in the “Bega” or dry season and a drop of up to 57.7% in the “Belg” or intermediate season in the projected A1B scenario. In the RCP precipitation rises up to 55.3% in Bega and drops to -65.4% in the Belg season. Precipitation data from 1965 to 2002 revealed a declining trend in its intensity in the eastern and southern parts of Ethiopia (Seleshi & Camberlin, 2006). Various studies in the Blue Nile basin reported varying precipitation changes in the future. Of the 17 GCMs analyzed in the study, 10 GCMs showed a decreasing trend in precipitation in the Blue Nile Basin (Elshamy et al., 2009). On the contrary, Beyene et al. (2010) used 11 GCM outputs and reported an increase in anticipated precipitation in the late twenty-first century in the Nile River Basin.

Seasonal changes in anticipated precipitation are more pronounced than annual changes in the watershed. Climate change predictions indicate that by

2050, East Africa will show a 5 – 10% drop and a 5 – 20% rise in rainfall between June to August and December to February respectively (IPCC, 2001). Similarly, Gebrechorkos et al. (2019) reported that precipitation is expected to decline up to -250 mm between the months of June and September. A study in the upper Gilgel Abay watershed in Ethiopia revealed an increase in rainfall in the climate predictions with mean annual rainfall variation less than mean monthly and seasonal variations (Adem et al., 2016). The rainfall pattern has a noteworthy seasonality, with dry season rainfall likely to rise and rainy season rainfall likely to decline in the Main Beles and Gilgel Beles sub-basins, Ethiopia (Worqlul et al., 2018). In a dry season, the expected increase in precipitation is greater than in a wet season, which means that smaller rainfall months (October, November, and December) are predicted to have a large precipitation increase, whereas high rainfall months (June, July, August, and September) are expected to see smaller precipitation decrease in the Rib watershed.

Prediction of temperature

The predicted rise in maximum and minimum temperatures in the A1B of this study ranges between 1.3 – 4.1 and 1.3 – 3.82 °C sequentially. In the RCPs, the rise in maximum temperature is between 1.35 and 4.7 °C and the minimum temperature is between 1.48 and 4.67 °C. Climate estimates of the twenty-first century showed that Africa’s land surface temperatures will increase faster than the global average, especially in arid environments (Niang et al., 2014). In the RCP8.5, Africa’s average annual temperature might increase between 3 and 6 °C by the end of the twenty-first century (Ofori et al., 2021).

In general, this study is in line with other studies in Ethiopia. In the significant portion of Ethiopia, minimum and maximum temperatures might increase by 6.1 °C and 4.3 °C respectively at the end of the twenty-first century (Gebrechorkos et al., 2019). From outputs of GCMs, Shiferaw et al. (2018) reported a high change in temperature in the RCP8.5 in the Ilala watershed, Ethiopia. The trend and rise in maximum and minimum temperatures in this study are consistent with the IPCC report and other studies. Climate change studies in Ethiopia reported an increase in future temperatures. A study on climate change in Ethiopia by GFDRR (2011) indicated

that the annual temperature is expected to increase between 1.1 and 3.1 °C in the 2060s and 1.5 and 5.1 °C in the 2090s. According to Girma (2012), the annual temperature in the upper Blue Nile basin will rise by 1.5 °C, 2.6 °C, and 4.5 °C between 2011 to 2040, 2041 to 2070, and 2071 to 2100, respectively. Elshamy et al. (2009) also reported that the predicted temperature in the Blue Nile Basin will increase between 2 and 5 °C.

Impacts of climate and LULC changes on hydrological components and sediment yield

For sustained water utilization and management, differentiating the long-term alterations in hydrological conditions produced by the distinct and coupled impacts of climate change and LULC change is critical. The expected changes in annual temperature and precipitation under A1B and RCPs created considerable variations in the future hydrology of the Rib watershed. SWAT simulations indicated that as precipitation decreases and temperatures rise, lateral flow, groundwater flow, and overall water output decreases in the RCPs and A1B, whereas surface runoff decreases in the A1B and increases in RCPs. Increased potential evapotranspiration which results from the rise in temperature could be a key reason for the declining water production in the watershed. The increase in surface runoff and decline in lateral flow and groundwater flow are due to the great loss of vegetation even in the base period. Groundwater and total water output reductions could have an impact on the availability of water resources in the watershed, exacerbating water stress farther downstream. Decreased soil moisture, which is readily available to plants and groundwater storage, could result from an increase in potential evapotranspiration (PET) caused by high temperatures combined with decreased precipitation. This means that there would be less water available for crop production, which will be a persistent problem for farmers of the watershed who rely only on agriculture for their living. The findings of this study agree with those of Beyene et al. (2010), who predicted that the Nile River will fall in the mid to late twenty-first century due to decreased precipitation and increased evaporation demand. In agreement with the present study, researchers reported that climate change has an influence on the Nile River basin's water resources. According to Coffel et al.

(2019), hot and dry years will be more common in the upper Nile as a result of rising regional temperatures, which could disrupt the region's water balance and result in a water deficit in the future. Serdeczny et al. (2017) verified the implications of future climate change in Sub-Saharan Africa, which results in the more recurrent occurrence of high warm and changes in rainfalls.

Under a dynamic LULC change, an increase in temperature and a decrease in precipitation in the Rib watershed results in increased surface runoff and evapotranspiration, as well as decreased groundwater flow and total water output. The climatic projections of the Rib watershed revealed a general decrease and increase in surface runoff, with certain variances in the A1B and RCPs, respectively. Its range is from -4.1 to +23.5.9% in RCPs and drops between 10. and 42.7% in A1B in the climate change scenarios, owing primarily to precipitation decline and the rising evaporation because of increased temperature. In the joint LULC change and climate change scenario, surface runoff declined between 5.6 and 39.6% in A1B and increase up to 28.7% in RCPs. The increase of surface runoff with decreasing precipitation in the watershed is mainly related to the large-scale LULC changes, especially the loss of vegetation. The analysis of the LULC changes showed that shrublands and mixed forests decreased by 82.3% and 100%, respectively, in 2049 (Table 5). Even though precipitation has shown a decrease, the accelerated decline of the vegetation cover causes the increase of surface runoff in the watershed with the available rainfall. The infiltration capacity of soils is greatly reduced due to the loss of vegetation, which results in an increase in runoff. Due to the increasing population number of the area, the demand for agricultural lands is increasing over time which causes the massive loss of vegetation, especially the natural vegetation which has the capacity to reduce surface flows. Plant cover reduces runoff by declining the intensity of rain falling on the ground through their canopy and interception losses, increasing infiltration through their roots and biopores, and by improving topsoil water retention because of the deposition of organic litter (Saiz et al., 2015; Taniguchi, 1997). Surface runoff is higher in managed land use due to reduced soil infiltration rates. Similar studies were reported related to the impact

of climate change on rainfall and runoff processes. Favreau et al. (2009) found an increase in surface runoff threefold in Southwest Niger from 1970 to 1980, despite a 23% drop in rainfall, because of the large-scale conversion of natural savanna to agricultural fields. While rainfall decreased between 3.3 and 9.8% in RCP4.5 and between 6.8 and 16.2% in RCP8.5, streamflow increased by 10.4% and 11.5% in RCP4.5 and 10.8% and 12.4% in RCP8.5 in the 2050s and 2080s, respectively (Daba & you, 2020). In their study of climate change implications on water sources in the Werii watershed of Ethiopia, Gebremeskel and Kebede (2018) estimated a 14% decrease in surface runoff due to the installation of exclosures (allowing an area for vegetation growth) and soil and water management initiatives in the watershed. The widespread transformation of LULC to agriculture diminished soil permeability, lateral flow, and groundwater flow resulting in a significant decrease in the water output of the study watershed. In connection to this, Dibaba et al. (2020) observed the loss of springs and a drop in water flow in the Finchaa catchment as a result of massive changes in LULC which triggered the declining groundwater recharge. In relation to this (Legesse et al., 2003; Mango et al., 2011; Marhaento et al., 2017; Shawul et al., 2019) stated that the expanding cropland and urban centers at the expense of shrublands, forests, and grassland resulted in an increase in surface runoff and a decreased in groundwater recharge. Due to the elimination of vegetation, Dinka and Klik (2020) also found an increase in overall runoff and accompanying sediment output in the Lake Basaka reservoir of Ethiopia between 1980 and 2000. Shi et al. (2013) reported an increase in evapotranspiration and surface water owing to the cumulative effect of LULC conversion and climate change in the upper Huai River, China, which is attributable to rainfall variability and alterations in LULC, although the climate contribution is more pronounced than the LULC conversions.

On the other hand, the impact of climate change studies by Hailemariam (1999) using GCMs of the Canadian Climate Center Model (CCCM) and Geophysical Fluid Dynamics Laboratory (GFD3) with SRES scenarios indicated a decline in precipitation up to 2% and a drop in runoff of between 10 and 34% in the Awash River basin of Ethiopia. A study of the impact of land use and climate change by Serpa et al.

(2015) using the A1B and B1 emission scenarios revealed a decline in annual rainfall of between 8 and 12%, which resulted in a decline in streamflow in the two Mediterranean catchments at the end of the twenty-first century. In such circumstances, RCPs may offer greater predictive performance for climate change impact studies than SRES scenarios.

In this study, the conditions of the water balance components show a significant change during the 2090s (end of the twenty-first century). Except in the A1B and RCP8.5, surface runoff shows a high increase in the 2090s time slice (Tables 8 and 9). A higher decrease in lateral flow is projected in the 2090s of A1B and RCP8.5 than in other climate projections. In general, the climate predictions show a higher increase in evapotranspiration in the 2090s (Tables 8 and 9). The increase in evapotranspiration is related to the rising temperature in the watershed, which is highly linked to the decline in water output. In addition to the declining precipitation, the rising evapotranspiration is the probable reason for the decline in the total water output of the watershed. In this case, the water output lost in the watershed then goes in the form of evapotranspiration. While the 2090s of A1B show a higher decline in total water yield, the 2090s of RCP8.5 and the 2060s of RCP 2.6 and 4.5 show almost equivalent reductions (Tables 8 and 9). The findings of this study are compatible with those of earlier studies conducted in Ethiopia's upper Blue Nile basin. Prediction under RCP8.5 shows a rise in surface runoff by up to 14% and evapotranspiration by 27% by the end of the twenty-first century over the basin (Mengistu et al., 2021). They also stated that in RCP8.5 of the twenty-first century, the basin's overall water output is expected to fall by up to 22.7%. The decline in water yield was projected by Elshamy et al. (2009) (15%) and Cherie (2013) (61%), for the entire upper Blue Nile basin. According to their analysis, the drop in water output in the basin is related to the increased evapotranspiration owing to the rising temperature, declined precipitation, and the consequent declining recharge of groundwater because of decreased lateral flow. Increased evapotranspiration over the basin was also reported by Elshamy et al. (2009) (14%), Cherie (2013) (4.6%), Worqlul et al. (2018) (27.8%), and Haile et al. (2017) (8.6%) at the turn of the twenty-first century.

Increased warmth and evapotranspiration may result in water deficits in the watershed. Even though

the effect of climate change is more significant to the changing hydrological components and sediment yield in the watershed, the projected increasing trend of LULC change also plays a great role. Other researchers in various parts of the world have reported on the vulnerability of water balance components to climate change (Blanco-Gómez et al., 2019; Leta et al., 2016; Ospina-Noreña et al., 2017; Pham et al., 2015; Shi et al., 2013). Shi et al. (2013) found that the joint impact of climate (an increase in temperature and no significant change in precipitation) and LULC change decreased evapotranspiration, increased surface water, and streamflow in the Huai River, China. Blanco-Gómez et al. (2019) presented that the amount of water shows a decrease due to the predicted decreasing trend of precipitation and increasing average temperatures in the middle and end of the twenty-first century in the Guajoyo River Basin. Leta et al. (2016) also analyzed the general decline in water balance components due to the decline in predicted rainfall, especially in the wet season. Pham et al. (2015) revealed that a decrease in streamflow is observed because of the changes in projected precipitation and potential evapotranspiration in the catchments of New Zealand. In the same manner, Ospina-Noreña et al. (2017) reported the projected increase in temperature and decrease in precipitation that resulted in the prospective decrease in the water balance of the Uribia-Guajira region of Colombia. The increase in surface runoff, mainly due to the dramatic LULC changes, reduces soil water infiltration and soil moisture required for crop growth, which may threaten the larger population depending on crop production in the Rib watershed.

In general, in FCC&FLULCC and FCC scenarios, sediment outputs show an increase in the watershed with the biggest rise occurring in the 2090s of RCP8.5 in the present study. In the 2090s of RCP8.5, it increased by up to 64% and 82% in the FCC and FLULCC&FCC scenarios, correspondingly. Sediment yield is increasing due to increased surface runoff and declining vegetation because of LULC changes, which result in a loss of soil nutrients for crop production. The removal of vegetation for farming purposes, which increases the speed of runoff and the amount of soil erosion on the sloppy and adulating terrain of the watershed, is the main contributing factor to the expected rise in sediment yield. Increased sediment output with decreased

precipitation, as seen in the Rib watershed, is comparable to what has been observed in previous studies (Khoi & Suetsugi, 2014; Li et al., 2012; Nunes et al., 2008). Rodríguez-Blanco et al. (2016) discovered an increase in sediment transport (11–17%) during winter, which they attribute to increased erosion in farming areas, which intensified soil detachment and removal. Azim et al. (2016) also revealed that future climate change is altering the Naran watershed, contributing to increased river discharge and suspended sediment output. These comparisons demonstrate the site-specific variability in the projected influence of climate and LULC changes, highlighting the necessity for specific instance impact studies that take into account the diversity of site-specific circumstances found in various locations (Smetanova et al., 2018).

However, contrary to the current analysis, there are several studies that show a drop in sediment output as a result of expected precipitation decreases in numerous catchments around the world. Gadissa et al. (2018) reported a 38% decline in annual sediment output in RCP4.5 and a 23% drop in RCP8.5 throughout 2041–2070 in the central Rift Valley of Ethiopia, which could be connected to a decrease in streamflow because of reduced precipitation. Many researchers have found variations in sediment yield in relation to changes in streamflow caused by climate change (Azari et al., 2016; Azim et al., 2016). According to Serpa et al. (2015), yearly sediment export has decreased by 9–11%, which could be attributed to lower precipitation and the cultivation of more soil-protective crops in the area, which is in contrast to the rising sediment loss in the Rib watershed. In similar research, annual sediment loads in the Maumee watershed declined by 23.5% and 3.3% in response to climate change under RCP4.5 and RCP8.5, respectively, in the middle of the twenty-first century (2046–2065) (Cousino et al., 2015). In southwest China, a report by Li et al. (2016) estimated an annual rate of reduction of water and sediment outflows that were often governed by climate variability. Rodríguez-Blanco et al. (2016) reported that owing to reduced streamflow as a result of climate change, suspended sediment is anticipated to drop by 11% from 2031 to 2060 and by 8% from 2069 to 2098. Choukri et al. (2020) concluded that the joint impact of climate and land-use change has resulted in a decrease in annual water and sediment supply in the Tleta watershed of Morocco. They pointed out that the

cumulative effect of changes in climate and land-use on water and sediment reaching the reservoir resulted in more significant changes than if the land-use and climate effects are examined separately.

In the FCC scenario, groundwater flow decreased by 6.7% to 52.5%, while in the FCC&FLULCC change scenario, it decreased by 7.1% to 53.3% in the study watershed. The variation in lateral flow is between 3.5 and -31% in the FCC scenario, and between -3.7 and -35.4% in the FCC&FLULCC scenario. The 2090s of A1B and RCP8.5 predicted a marked decline in lateral flow compared to other climatic periods. The substantial replacement of vegetation by farmlands could be the primary reason for the diminishing water recharge. The findings are in line with those of other research conducted across the country. For example, Gashaw et al. (2018) found that changes in land use had drastically reduced groundwater flow in the Andassa catchment. According to Shawul et al. (2019), the development of agriculture and urban areas, as well as the degradation of forests, shrublands, and pastures, diminished groundwater flow and lateral flow in Ethiopia's upper Awash basin. Marhaento et al. (2017) revealed that the expanding settlements have resulted in a reduced ratio of groundwater recharge in the Samin River catchment.

Future projections show an increase in evapotranspiration, peaking at 19.2% in the 2090s of RCP predictions, resulting in a decrease in total water production for this study (Table 9). In the future, both the rise in evapotranspiration and the decline in precipitation will contribute to the deficit in total water production of the watershed. The overall water yield declines by up to 9.9% and 47.3% in RCPs and A1B sequentially in the FCC scenario and by up to 9.5% and 47% in RCPs and A1B respectively in the FLULCC&FCC scenario (Tables 8 and 9). The findings are consistent with previous research in Ethiopian catchments. In this context, Mengistu et al. (2021) reported a 22.7% decline in the overall water output in RCP8.5 in the upper Blue Nile basin due to the 27% rise in evapotranspiration by the turn of the twenty-first century. A drop of 15% and 61% in water output is reported by Elshamy et al. (2009) and Cherie (2013) sequentially in the upper Blue Nile basin because of the rising evapotranspiration as a result of increasing temperatures, decreasing precipitation, and the consequent declining groundwater recharge. At the turn of this century, the basin's increasing evapotranspiration is reported

between 2.8 and 14% (Cherie, 2013; Elshamy et al., 2009; Haile et al., 2017; Worqlul et al., 2018). While climate change has a significant implication on water balance components, LULC modifications have a massive effect on the sediment output of the watershed. The decline in water output, primarily owing to the conversion of vegetation to agriculture (LULC alterations) and increased evaporation, affects water infiltration and soil moisture essential for crop growth, jeopardizing the population in the watershed who rely on crop production. Sediment yield is growing as a result of falling vegetation due to LULC alterations, leading to a loss of soil quality for crop production, which is endangering the food security of the people of the area.

Conclusions

The climate prediction (2025–2099) showed that there might be a decrease in rainfall and an increase in temperature in the watershed. The LULC prediction (2016–2049) indicated that there is an increase in cultivation land at the expense of native vegetation. The decrease of native vegetation resulted in an increase in surface runoff in the RCP periods. Surface runoff is higher in the FLULCC&FCC scenario than in the FCC scenario. There might be a general decrease in lateral flow, groundwater flow, and total water yield in A1B and RCP scenarios, with the highest decrease in the A1B time slices. Lateral flow and groundwater flow might show a higher decrease in the FLULCC&FCC than in the FCC scenario. The decrease in total water yield did not show significant variation amongst the scenarios. The increase in ET is higher in the RCPs than in the A1B periods. A little higher value of ET is shown in the FCC scenario which might be due to the better vegetation cover than in the FLULCC&FCC scenario. Sediment yield is expected to show an increase except in the 2060s and 2090s of RCP2.6 and A1B periods. A significant decrease may occur in the A1B time slices. In general, sediment yield is expected to show a high increase in the FLULCC&FCC scenario, which is attributed to the expansion of cultivated lands. Reports from the Ethiopian Highlands indicate that an increase in sediment yield is attributed to an increase in crop cultivation. From this study, it is found that both the changing LULC and climate have a significant impact on the hydrological response of the watershed. The

results of this study indicated that future predictions of water balance components through combining the predicted changes of LULC conditions by employing appropriate LULC modeling tools and climate variables from the climate models could be an important input for future water and land management planning. The prediction of the status of the water balance components could be a vital input for the management and proper utilization of the water resources of the area. In addition, the prediction of the status of the water balance components provides understanding and direction for land resource managers and experts to design and implement appropriate land management methods that help to cope with the changing climate, LULC, and water resources in the area. The study has limitations to including other models of land use prediction and more RCM outputs in the impact analysis for comparisons of the results. To find the best results and to better understand the present and cope with future conditions, further studies incorporating varieties of land use and climate prediction models are recommended. Lastly, we recommend that in watershed impact studies, researchers have to incorporate the LULC change scenarios together with the climate change scenarios to acquire a comprehensive picture of the hydrologic response of watersheds.

Acknowledgements We express our gratitude to Bahir Dar University for its grant support for the work. We also express our heartfelt gratitude to Ethiopian Meteorological Agency (EMA) for providing meteorological data and the Ministry of Water Resource of Ethiopia for flow, sediment, and soil data used to accomplish this study.

Funding This work was supported by Bahir Dar University (BDU), Ethiopia.

Availability of data and material Not applicable.

Code availability Not applicable.

Declarations

Conflict of interest The authors declare no conflict of interest.

References

- Abbaspour, K. C., Rouholahnejad, E., Vaghefi, S., Srinivasan, R., Yang, H., & Kløve, B. (2015). A continental-scale hydrology and water quality model for Europe: Calibration and uncertainty of a high-resolution large-scale SWAT model. *Journal of Hydrology*, 524, 733–752. <https://doi.org/10.1016/j.jhydrol.2015.03.027>
- Abbaspour, K. C. (2013). *SWAT-CUP 2012: SWAT calibration and uncertainty programs—A user manual*. Eawag, Dübendorf, Switzerland, pp. 103.
- Abe, C., Lobo, F., Dibike, Y., Costa, M., Dos Santos, V., & Novo, E. (2018). Modelling the effects of historical and future land cover changes on the hydrology of an amazonian basin. *Water*, 10(7), 932. <https://doi.org/10.3390/w10070932>
- Abdo, K. S., Fiseha, B. M., Rientjes, T. H. M., Gieske, A. S. M., & Haile, A. T. (2009). Assessment of climate change impacts on the hydrology of Gilgel Abay catchment in Lake Tana basin, Ethiopia. *Hydrological Processes*, 23(26), 3661–3669. <https://doi.org/10.1002/hyp.7363>
- Addor, N., Rössler, O., Köplin, N., Huss, M., Weingartner, R., & Seibert, J. (2014). Robust changes and sources of uncertainty in the projected hydrological regimes of Swiss catchments. *Water Resources Research*, 50(10), 7541–7562. <https://doi.org/10.1002/2014WR015549>
- Adem, A. A., Tilahun, S. A., Ayana, E. K., Worqlul, A. W., Assefa, T. T., Dessu, S. B., & Melesse, A. M. (2016). Climate change impact on sediment yield in the Upper Gilgel Abay catchment, Blue Nile Basin, Ethiopia. In *Proc., Landscape dynamics, soils and hydrological processes in varied climates*. Springer Geography. https://doi.org/10.1007/978-3-319-18787-7_28
- Akbari, H., Mesbahzadeh, T., & Zehtabian, G. (2021). Prediction of climate change in arid and semi-arid regions of the western basin of Jazmourian Wetland. *Environmental Erosion Research Journal*, 11(3), 27–43.
- Alemseged, T. H., & Tom, R. (2015). Evaluation of regional climate model simulations of rainfall over the Upper Blue Nile basin. *Atmospheric Research*, 161, 57–64. <https://doi.org/10.1016/j.atmosres.2015.03.013>
- Amsalu, A., Stroosnijder, L., & de Graaff, J. (2007). Long-term dynamics in land resource use and the driving forces in the Beressa watershed, highlands of Ethiopia. *Journal of Environmental Management*, 83, 448–459. <https://doi.org/10.1016/j.jenvman.2006.04.010>
- Anand, J., Gosain, A. K., Khosa, R., & Srinivasan, R. (2018). Regional scale hydrologic modeling for prediction of water balance, analysis of trends in streamflow and variations in streamflow: The case study of the Ganga River basin. *Journal of Hydrology: Regional Studies*, 16, 32–53. <https://doi.org/10.1016/j.ejrh.2018.02.007>
- Arnold, J. G., Kiniry, J. R., Srinivasan, R., Williams, J. R., Haney, E. B., & Neitsch, S. L. (2012). *SWAT input/output documentation version 2012*, Vol.654. Texas Water Resources Institute, pp 1–646.
- Arnold, J. G., Srinivasan, R., Mutiah, R. S., & Williams, J. R. (1998). Large area hydrologic modeling and assessment part I: Model development. *Journal of the American Water Resources Association*, 34(1), 73–89. <https://doi.org/10.1111/j.1752-1688.1998.tb05961.x>
- Arsanjani, J. J., Helbich, M., Kainz, W., & Boloorani, A. D. (2013). Integration of logistic regression, Markov chain and cellular automata models to simulate urban expansion. *International Journal of Applied Earth Observation and Geoinformation*. <https://doi.org/10.1016/j.jag.2011.12.014>

- Azari, M., Moradi, H. R., Saghafian, B., & Faramarzi, M. (2016). Climate change impacts on streamflow and sediment yield in the North of Iran. *Hydrological Sciences Journal*, 61(1), 123–133. <https://doi.org/10.1080/02626667.2014.967695>
- Azim, F., Shakir, A. S., & Kanwal, A. (2016). Impact of climate change on sediment yield for Naran watershed, Pakistan. *International Journal of Sediment Research*, 31(3), 212–219. <https://doi.org/10.1016/j.ijsrc.2015.08.002>
- Bates, B., Kundzewicz, Z., & Wu, S. (2008). *Climate change and water. Technical Paper Intergovernmental Panel on Climate Change*, IPCC Secretary, Geneva, pp210.
- Berihun, M. L., Tsunekawa, A., Haregeweyn, N., Meshesha, D. T., Adgo, E., Tsubo, M., Ebabu, K., et al. (2019). Hydrological responses to land use/land cover change and climate variability in contrasting agro-ecological environments of the Upper Blue Nile basin, Ethiopia. *Science of the Total Environment*, 689, 347–365. <https://doi.org/10.1016/j.scitotenv.2019.06.338>
- Bewket, W. (2002). Land cover dynamics since the 1950s in Chemoga watershed, Blue Nile basin, Ethiopia. *Mountain Research and Development*, 22(3), 263–270. [https://doi.org/10.1659/0276-4741\(2002\)022\[0263:LCDSTI\]2.0.CO;2](https://doi.org/10.1659/0276-4741(2002)022[0263:LCDSTI]2.0.CO;2)
- Beyene, T., Lettenmaier, D. P., & Kabat, P. (2010). Hydrologic impacts of climate change on the Nile River Basin: Implications of the 2007 IPCC scenarios. *Climate Chang*, 100, 433–461. <https://doi.org/10.1007/s10584-009-9693-0>
- Blanco-Gómez, P., Jimeno-Sáez, P., Senent-Aparicio, J., & Pérez-Sánchez, J. (2019). Impact of climate change on water balance components and droughts in the Guajoyo River Basin (El Salvador). *Water*, 11(11), 2360. <https://doi.org/10.3390/w11112360>
- BoEPLAU. (2015). *Tana sub-basin integrated land use planning and environmental impact study project. Technical report: Land use land cover and change detection*. Bahir Dar, Ethiopia.
- Borgomeo, E., Vadheim, B., Woldeyes, F. B., Alamirew, T., Tamru, S., Charles, K. J., Kebede, S., & Walker, O. (2018). The distributional and multi-sectoral impacts of rainfall shocks: Evidence from computable general equilibrium modelling for the Awash Basin, Ethiopia. *Ecological Economics*, 146, 621–632. <https://doi.org/10.1016/j.ecolecon.2017.11.038>
- Bosshard, T., Kotlarski, S., Ewen, T., & Schär, C. (2011). Spectral representation of the annual cycle in the climate change signal. *Hydrology and Earth System Sciences*, 15(9), 2777–2788. <https://doi.org/10.5194/hess-15-2777-2011>
- Braimoh, A. K., & Vlek, P. L. G. (2005). Land-cover change trajectories in Northern Ghana. *Environmental Management*, 36(3), 356–373. <https://doi.org/10.1007/s00267-004-0283-7>
- Brands, S., Herrera, S., Fernández, J., & Gutiérrez, J. M. (2013). How well do CMIP5 Earth System Models simulate present climate conditions in Europe and Africa? *Climate Dynamics*, 41(3–4), 803–817. <https://doi.org/10.1007/s00382-013-1742-8>
- Chen, Y., & Yu, B. (2013). Impacts of climate and land-use changes on floods in an urban catchment in southeast Queensland, Australia. In *Proc., Climate and Land Surface Changes in Hydrology*. IAHS-IAPSO-IASPEI Assembly, Gothenburg, Sweden, IAHS Press.
- Cherie, N. Z. (2013). Downscaling and modeling the effects of climate change on hydrology and water resources in the Upper Blue Nile River Basin, Ethiopia. PhD dissertation, University of Kassel, Germany.
- Choukri, F., Raclot, D., Naimi, M., Chikhaoui, M., Nunes, J. P., Huard, F., Hérivaux, C., Sabir, M., & Pépin, Y. (2020). Distinct and combined impacts of climate and land use scenarios on water availability and sediment loads for a water supply reservoir in northern Morocco. *International Soil and Water Conservation Research*, 8(2), 141–153. <https://doi.org/10.1016/j.iswcr.2020.03.003>
- Coffel, E. D., Keith, B., Lesk, C., Horton, R. M., Bower, E., Lee, J., & Mankin, J. S. (2019). Future hot and dry years worsen Nile Basin water scarcity despite projected precipitation increases. *Earth's Future*, 7(8), 967–977. <https://doi.org/10.1029/2019EF001247>
- Collier, P., Conway, G., & Venables, T. (2008). Climate change and Africa. *Oxford Review of Economic Policy*, 24, 337–353. <https://doi.org/10.1093/oxrep/grn019>
- Congalton, R. G., & Green, K. (1999). *Assessing the accuracy of remotely sensed data: Principles and practices*. Lewis Publishers.
- Conway, T. M., & Lathrop, R. G. J. (2005). Modeling the ecological consequences of land-use policies in an urbanizing region. *Environmental Management*, 35, 278–291. <https://doi.org/10.1007/s00267-004-4067-x>
- Conway, D., & Schipper, E. L. F. (2011). Adaptation to climate change in Africa: Challenges and opportunities identified from Ethiopia. *Global Environmental Change*, 21(1), 227–237. <https://doi.org/10.1016/j.gloenvcha.2010.07.013>
- Cousino, L. K., Becker, R. H., & Zmijewski, K. A. (2015). Modeling the effects of climate change on water, sediment, and nutrient yields from the Maumee River watershed. *Journal of Hydrology: Regional Studies*, 4, 762–775. <https://doi.org/10.1016/j.ejrh.2015.06.017>
- Daba, M. H., & You, S. (2020). Assessment of climate change impacts on river flow regimes in the upstream of Awash Basin, Ethiopia: Based on IPCC fifth assessment report (AR5) climate change scenarios. *Hydrology*, 7(4), 98. <https://doi.org/10.3390/hydrology7040098>
- Dibaba, W. T., Demissie, T. A., & Miegel, K. (2020). Drivers and implications of land use/land cover dynamics in Finchaa catchment, Northwestern Ethiopia. *Land*, 9, 113. <https://doi.org/10.3390/land9040113>
- Dinka, M. O., & Klik, A. (2020). Temporal and spatial dynamics of surface run-off from Lake Basaka catchment (Ethiopia) using SCS-CN model coupled with remote sensing and GIS. *Lakes & Reservoirs: Research & Management*, 25(2), 167–182. <https://doi.org/10.1111/lre.12313>
- D’oll, P., Jiméneiz-Cisneros, B., Oki, T., Arnell, N. W., Benito, G., Cogley, J. G., Jiang, T., Kundzewicz, Z. W., Mwakalila, S., & Nishijima, A. (2015). Integrating risks of climate change into water management. *Hydrological Sciences Journal*, 60(1), 4–13. <https://doi.org/10.1080/02626667.2014.967250>
- Dos Santos, V., Laurent, F., Abe, C., & Messner, F. (2018). Hydrologic response to land use change in a large basin in Eastern Amazon. *Water*, 10(4), 429. <https://doi.org/10.3390/w10040429>
- Elshamy, M. E., Seierstad, I. A., & Sorteberg, A. (2009). Impacts of climate change on Blue Nile flows using

- bias-corrected GCM scenarios. *Hydrology and Earth System Sciences*, 13, 551–565. <https://doi.org/10.5194/hess-13-551-2009>
- ENMA. (2007). *Climate Change National Adaptation Programme of Action (NAPA) of Ethiopia*. p1–73. Addis Ababa, Ethiopia. <https://www.climatelearningplatform.org/ethiopia-national-programme-action-napa>
- Erdoğan, N., Nurlu, E., & Erdem, Ü. (2011). Modelling land use changes in Karaburun by using CLUE-s. *AIZ ITU Journal of the Faculty of Architecture*, 8(2), 91–102.
- FAO-IPCC. (2017). *FAO-IPCC Expert meeting on climate change, land use and food security. Final Meeting report*. Rome, FAO and IPCC.
- Faramarzi, M., Abbaspour, K. C., Vaghefi, S. A., Farzaneh, M. R., Zehnder, A. J., Srinivasan, R., & Yang, H. (2013). Modeling impacts of climate change on freshwater availability in Africa. *Journal of Hydrology*, 480, 85–101. <https://doi.org/10.1016/j.jhydrol.2012.12.016>
- Favreau, G., Cappelaere, B., Massuel, S., Leblanc, M., Boucher, M. N., Boulain, N., & Leduc, C. (2009). Land clearing, climate variability, and water resources increase in semiarid southwest Niger: A review. *Water Resources Research*, 45, W00A16. <https://doi.org/10.1029/2007WR006785>
- Fazzini, M., Bisci, C., & Billi, P. (2015). The Climate of Ethiopia. In P. Billi (Ed.), *Landscapes and Landforms of Ethiopia, World Geomorphological Landscapes* (pp. 65–87). Springer, Dordrecht. https://doi.org/10.1007/978-94-017-8026-1_3
- Feyen, J., & Raul, F. V. (2011). Modeling hydrological consequences of climate and land use change - progress and challenges. *Maskana*, 2(2), 83–100. <https://orcid.org/0000-0002-2334-6499>
- Fowler, H. J., Blenkinsop, S., & Tebaldi, C. (2007). Review: Linking climate change modelling to impacts studies: Recent advances in downscaling techniques for hydrological modeling. *International Journal of Climatology*, 27, 1547–1578. <https://doi.org/10.1002/joc.1556>
- Funk, C., Senay, G., Asfaw, A., Verdin, J., Rowland, J., Michaelsen, J., Eilerts, G., Korecha, D., & Choularton, R. (2005). Recent drought tendencies in Ethiopia and equatorial-subtropical eastern Africa. *FEWS Report*, 1, 13.
- Gadissa, T., Nyadawa, M., Behulu, F., & Mutua, B. (2018). The effect of climate change on loss of lake volume: Case of sedimentation in central rift valley basin, Ethiopia. *Hydrology*, 5(4), 67. <https://doi.org/10.3390/hydrology5040067>
- Gashaw, T., Tulu, T., Argaw, M., Worqlul, A. W., Tolessa, T., & Kindu, M. (2018). Estimating the impacts of land use/land cover changes on ecosystem service values: The case of the Andassa watershed in the Upper Blue Nile basin of Ethiopia. *Ecosystem Services*. [https://doi.org/10.1016/j.ecoser.2018.05.001.31\(June\)](https://doi.org/10.1016/j.ecoser.2018.05.001.31(June))
- Gassman, P. W., Reyes, M. R., Green, C. H., & Arnold, J. G. (2007). The soil and water assessment tool: Historical development, applications and future directions. *Trans ASABE*, 50(4), 1211–1250. <https://doi.org/10.13031/2013.23637>
- Gebrechorkos, S. H., Hülsmann, S., & Bernhofer, C. (2019). Regional climate projections for impact assessment studies in East Africa. *Environmental Research Letters*, 14(4), 044031. <https://doi.org/10.1088/1748-9326/ab055a>
- Gebremeskel, G., & Kebede, A. (2018). Estimating the effect of climate change on water resources: Integrated use of climate and hydrological models in the Werii watershed of the Tekeze river basin, Northern Ethiopia. *Agriculture and Natural Resources*, 52(2), 195–207. <https://doi.org/10.1016/j.anres.2018.06.010>
- Gbobaniyi, E., Sarr, A., Sylla, M. B., Diallo, I., Lennard, C., Dosio, A., Dhiédiou, A., Kamga, A., Klutse, N. A. B., Hewitson, B., Nikulin, G., & Lamptey, B. (2014). Climatology, annual cycle and interannual variability of precipitation and temperature in CORDEX simulations over West Africa. *International Journal of Climatology*, 34, 2241–2257. <https://doi.org/10.1002/joc.3834>
- GFDRR. (2011). *Climate risk and adaptation country profile: Ethiopia*; World Bank: Washington, DC.
- Girma, M. M. (2012). *Potential impact of climate and land use changes on the water resources of the Upper Blue Nile Basin*. Freie Universität.
- Graham, L. P., Andréasson, J., & Carlsson, B. (2007). Assessing climate change impacts on hydrology from an ensemble of regional climate models, model scales and linking methods—a case study on the Lule River basin. *Climatic Change*, 81(1), 293–307. <https://doi.org/10.1007/s10584-006-9215-2>
- Hagen, A. (2003). Fuzzy set approach to assessing similarity of categorical maps. *International Journal of Geographical Information Science*, 17, 235–249. <https://doi.org/10.1080/13658810210157822>
- Haile, A. T., Akawka, A. L., Berhanu, B., & Rientjes, T. (2017). Changes in water availability in the Upper Blue Nile basin under the representative concentration pathways scenario. *Hydrological Sciences Journal*, 62(13), 2139–2149. <https://doi.org/10.1080/02626667.2017.1365149>
- Hailemariam, K. (1999). Impact of climate change on the water resources of Awash River Basin, Ethiopia. *Climate Research*, 12(2–3), 91–96.
- Hattermann, F. F. (2011). *Re-thinking water storage in Sub-Saharan Africa, report on generation of regional climate scenarios*. Center for Development Research, University of Burn.
- Hewitt, R., & Escobar, F. (2011). The territorial dynamics of fast-growing regions: Unsustainable land use change and future policy challenges in Madrid, Spain. *Applied Geography*, 31, 650–667. <https://doi.org/10.1016/j.apgeog.2010.11.002>
- Houessou, L. G., Tekla, O., Imorou, I. T., Lykke, A. M., & Sinsin, B. (2013). Land use and land-cover change at “W” biosphere reserve and its surroundings areas in Benin Republic (West Africa). *Environment and Natural Resources Research*, 3(2), 87–101. <https://doi.org/10.5539/enrr.v3n2p87>
- Hyandye, C. B., Worqlul, A., Martz, L. W., & Muzuka, A. N. (2018). The impact of future climate and land use/cover change on water resources in the Ndembera watershed and their mitigation and adaptation strategies. *Environmental Systems Research*, 7(1), 1–24. <https://doi.org/10.1186/s40068-018-0110-4>
- IPCC. (2001). *Climate change 2001: The scientific basis. Contribution of Working Group I to the Third Assessment Report of the Intergovernmental Panel on Climate Change*, Houghton J. T., Ding Y., Griggs D. J., Noguer

- M., van der Linden P. J., Dai X., Maskell K., & Johnson C. A. (eds.), Cambridge University Press, Cambridge, United Kingdom and New York, NY, USA, 881pp.
- IPCC. (2007). *Climate change 2007: Synthesis report. Contribution of Working Groups I, II and III to the Fourth Assessment Report of the Intergovernmental Panel on Climate Change*. Pachauri R. K., Reisinger A. (eds.), (pp. 104). IPCC, Geneva, Switzerland.
- IPCC. (2014). *Climate change 2014: Synthesis report. Contribution of Working Groups I, II and III to the Fifth Assessment Report of the Intergovernmental Panel on Climate Change*. Pachauri R. K., Meyer L. A. (eds.), (pp.151). IPCC, Geneva, Switzerland.
- Irwin, E. G., & Geoghegan, J. (2001). Theory, data, methods: Developing spatially explicit economic models of land use change. *Agriculture, Ecosystems & Environment*, 85(1–3), 7–24. [https://doi.org/10.1016/S0167-8809\(01\)00200-6](https://doi.org/10.1016/S0167-8809(01)00200-6)
- Kassa, T. (2009). *Watershed hydrological responses to changes in land use and land cover, and management practices at Hare Watershed, Ethiopia*. Doctoral dissertation, University of Siegen, Research Institute for water and Environment, Siegen, Germany.
- Khoi, D. N., & Suetsugi, T. (2014). The responses of hydrological processes and sediment yield to land-use and climate change in the Be River Catchment, Vietnam. *Hydrological Processes*, 28, 640–652.
- Lagrosa, J. J., Zipperer, W. C., & Andreu, M. G. (2018). Projecting land-use and land cover change in a subtropical urban watershed. *Urban Science*, 2(1), 11. <https://doi.org/10.3390/urbansci2010011>
- Lambin, E. F., Rounsevell, M. D. A., & Geist, H. J. (2000). Are agricultural land use models able to predict changes in land-use intensity? *Agriculture, Ecosystems & Environment*, 82, 321–331. [https://doi.org/10.1016/S0167-8809\(00\)00235-8](https://doi.org/10.1016/S0167-8809(00)00235-8)
- Legesse, D., Vallet-Coulomb, C., & Gasse, F. (2003). Hydrological response of a catchment to climate and land use changes in Tropical Africa: Case study south central Ethiopia. *Journal of Hydrology*, 275, 67–85. [https://doi.org/10.1016/S0022-1694\(03\)00019-2](https://doi.org/10.1016/S0022-1694(03)00019-2)
- Leroux, S. J., Albert, C. H., Lafuite, A. S., Rayfield, B., Wang, S., & Gravel, D. (2017). Structural uncertainty in models projecting the consequences of habitat loss and fragmentation on biodiversity. *Ecography*, 40, 36–47. <https://doi.org/10.1111/ecog.02542>
- Leta, O. T., El-Kadi, A. I., Dulai, H., & Ghazal, K. A. (2016). Assessment of climate change impacts on water balance components of Heeia watershed in Hawaii. *Journal of Hydrology: Regional Studies*, 8, 182–197. <https://doi.org/10.1016/j.ejrh.2016.09.006>
- Li, H., Zhang, Y., Vaze, J., & Wang, B. (2012). Separating effects of vegetation change and climate variability using hydrological modelling and sensitivity-based approaches. *Journal of Hydrology*, 420–421, 403–418. <https://doi.org/10.1016/j.jhydrol.2011.12.033>
- Li, Z., Xu, X., Yu, B., Xu, C., Liu, M., & Wang, K. (2016). Quantifying the impacts of climate and human activities on water and sediment discharge in a karst region of southwest China. *Journal of Hydrology*, 2016(542), 836–849. <https://doi.org/10.1016/j.jhydrol.2016.09.049>
- Lillesand, T. M., & Kiefer, R. M. (2004). Remote sensing and image interpretation (Fifth Edition). *Geographical Journal*, 146 (3). <https://doi.org/10.2307/634969>
- Lin, P. Y., Nien-Ming Hong, N. M., Pei-Jung, Wu, P. J., & Lin, C. J. (2007). Modeling and assessing land-use and hydrological processes to future land-use and climate change scenarios in watershed land-use planning. *Environmental Geology*, 53, 623–634. <https://doi.org/10.1007/s00254-007-0677-y>
- Luck, M., Landis, M., & Gassert, F. (2015). *Aqueduct water stress projections: Decadal projections of water supply and demand using CMP5 GCMs; Technical Note*; World Resources Institute: Washington, DC, USA. Pp.1–20. Available online: <https://www.wri.org/publication/aqueduct-water-stress-projections>. Accessed on 10 October 2021.
- Mandrekar, J. N. (2010). Receiver operating characteristic curve in diagnostic test assessment. *Journal of Thoracic Oncology*, 5, 1315–1316. <https://doi.org/10.1097/JTO.0b013e3181ec173d>
- Mango, L., Melesse, A., McClain, M. E., Gann, D., & Setegn, S. G. (2011). Land use and climate change impacts on the hydrology of the upper Mara River Basin, Kenya: Results of a modelling study to support better resource management. *Hydrology and Earth System Sciences*, 15(7), 2245–2258. <https://doi.org/10.5194/hess-15-2245-2011>
- Marhaento, H., Booij, M. J., Rientjes, T. H. M., & Hoekstra, A. Y. (2017). Attribution of changes in the water balance of a tropical catchment to land use change using the SWAT model. *Hydrological Processes*, 31, 2029–2040. <https://doi.org/10.1002/hyp.11167>
- Matata, P., Bushesha, M., & Msindai, J. (2019). Assessing rainfall and temperature changes in semi-arid areas of Tanzania. *American Journal of Climate Change*, 8(2), 173–189. <https://doi.org/10.4236/ajcc.2019.82010>
- Mendez, M., Maathuis, B., Hein-Griggs, D., & Alvarado-Gamboa, L. F. (2020). Performance evaluation of bias correction methods for climate change monthly precipitation projections over Costa Rica. *Water*, 12(2), 482. <https://doi.org/10.3390/w12020482>
- Mengistu, D., Bewket, W., Dosio, A., & Panitz, H. J. (2021). Climate change impacts on water resources in the Upper Blue Nile (Abay) River Basin, Ethiopia. *Journal of Hydrology*, 592, 125614. <https://doi.org/10.1016/j.jhydrol.2020.125614>
- Millington, J. D. A., Perry, G. L. W., & Romero-Calcerrada, R. (2007). Regression techniques for examining land use/cover change: a case study of a Mediterranean landscape. *Ecosystems*, 10(4), 562–578. <https://doi.org/10.1007/s10021-007-9020-4>
- Moore, K., Pierson, D., Pettersson, K., Schneiderman, E., & Samuelsson, P. (2008). Effects of warmer world scenarios on hydrologic inputs to Lake Mälaren, Sweden and implications for nutrient loads. *Hydrobiologia*, 599, 191–199. <https://doi.org/10.1007/s10750-007-9197-8>
- Moriasi, D. N., Arnold, J. G., Van Liew, M. W., Bingner, R. L., Harmel, R. D., & Veitch, T. L. (2007). Model evaluation guidelines for systematic quantification of accuracy in watershed simulations. *Transactions of the ASABE*, 50 (3), 885–900. <https://doi.org/10.13031/2013.23153>

- MoWR. (1998). *Abbay river basin integrated development master plan project. Phase 2: Data collection—site investigation survey and analysis*. Ethiopia.
- Neitsch, S. L., Williams, J. R., Arnold, J. G., & Kiniry, J. R. (2005). *Soil and water assessment tool—Theoretical documentation, version 2005*. Temple, Texas, USA.
- Niang, I., Ruppel, O.C., Abdrabo, M.A., Essel, A., Lennard, C., Padgham, J., & Urquhart, P. (2014). *Africa. Climate change 2014: impacts, adaptation, and vulnerability. Part B: regional aspects. Contribution of working group II to the fifth assessment report of the intergovernmental panel on climate change*, Barros V. R., Field C. B., Dokken D. J., Mastrandrea M. D., Mach K. J., Bilir T. E., Chatterjee M., Ebi K. L., Estrada Y. O., Genova R. C., Girma B., Kissel E. S., Levy A. N., MacCracken S., Mastrandrea P. R., & White L. L. (eds.), Cambridge University Press, Cambridge, pp 1199–1265.
- Nie, W. M., Yuan, Y. P., Kepner, W., Nash, M. S., Jackson, M., & Erickson, C. (2011). Assessing impacts of landuse changes on hydrology for the upper San Pedro watershed. *Journal of Hydrology*, 407, 105–114. <https://doi.org/10.1016/j.jhydrol.2011.07.012>
- Nunes, J. P., Seixas, J., & Pacheco, N. R. (2008). Vulnerability of water resources, vegetation productivity and soil erosion to climate change in Mediterranean watersheds. *Hydrological Processes*, 22(3115–866), 3134. <https://doi.org/10.1002/hyp.6897>
- Ofori, S. A., Cobbina, S. J., & Obiri, S. (2021). Climate change, land, water and food security: Perspectives from Sub-Saharan Africa. *Frontiers in Sustainable Food Systems*, 5, 218. <https://doi.org/10.3389/fsufs.2021.680924>
- Orlowsky, B., & Seneviratne, S. I. (2012). Global changes in extreme events: Regional and seasonal dimension. *Climatic Change*, 110, 669–696. <https://doi.org/10.1007/s10584-011-0122-9>
- Ospina-Noreña, J. E., Domínguez-Ramírez, C. A., Vega-Rodríguez, E. E., Darghan-Contreras, A. E., & Rodríguez-Molano, L. E. (2017). Analysis of the water balance under regional scenarios of climate change for arid zones of Colombia. *Atmósfera*, 30(1), 63–76. <https://doi.org/10.20937/ATM.2017.30.01.06>
- Panitz, H. J., Dosio, A., Büchner, M., Lüthi, D., & Keuler, K. (2014). COSMO-CLM (CCLM) climate simulations over CORDEXAfrica domain: Analysis of the ERA-interim driven simulations at 0.44° and 0.22° resolution. *Climate Dynamics*, 42, 3015–3038. <https://doi.org/10.1007/s00382-013-1834-5>
- Pham, H. X., Shamseldin, A. Y., & Melville, B. W. (2015). Assessment of climate change impact on water balance of forested and farmed catchments. *Journal of Hydrologic Engineering*, 20(10), 04015009. [https://doi.org/10.1061/\(ASCE\)JHE.1943-5584.0001169](https://doi.org/10.1061/(ASCE)JHE.1943-5584.0001169)
- Pontius, Jr.G.R., & Schneider, C.L. (2001). Land-cover change model validation by an ROC method for the Ipswich watershed, Massachusetts, USA. *Agriculture, Ecosystems & Environment*, 85, 239–248. [https://doi.org/10.1016/S0167-8809\(01\)00187-6](https://doi.org/10.1016/S0167-8809(01)00187-6)
- Pontius, R. G. Jr. (2000). Quantification error versus location error in comparison of categorical maps. *Photogrammetric Engineering & Remote Sensing*, 66(8), 1011–1016.
- Rientjes, T. H. M., Haile, A. T., Kebede, E., Mannaerts, C. M. M., Habib, E., & Steenhuis, T. S. (2011). Changes in land cover, rainfall and stream flow in Upper Gilgel Abay catchment, Blue Nile basin – Ethiopia. *Hydrology and Earth System Sciences*, 15, 1979–1989. <https://doi.org/10.5194/hess-15-1979-2011>
- Riahi, K., Rao, S., Krey, V., Cho, C., Chirkov, V., Fischer, G., Kindermann, G., Nakicenovic, N., & Rafaj, P. (2011). RCP 8.5 a scenario of comparatively high greenhouse gas emissions. *Climate Change*, 109, 33–57. <https://doi.org/10.1007/s10584-011-0149-y>
- Rodríguez-Blanco, M. L., Arias, R., Taboada-Castro, M. M., Nunes, J. P., Keizer, J. J., & Taboada-Castro, M. T. (2016). Sediment yield at catchment scale using the SWAT (Soil and Water Assessment Tool) model. *Soil Science*, 181(7), 326–334. <https://doi.org/10.1097/SS.0000000000000158>
- Rykiel, E. J. (1996). Testing ecological models: the meaning of validation. *Ecological Modelling*, 90(3), 229–244. [https://doi.org/10.1016/0304-3800\(95\)00152-2](https://doi.org/10.1016/0304-3800(95)00152-2)
- Sahin, V., & Hall, M. J. (1996). The effects of afforestation and deforestation on water yields. *Journal of Hydrology*, 178, 293–309. [https://doi.org/10.1016/0022-1694\(95\)02825-0](https://doi.org/10.1016/0022-1694(95)02825-0)
- Saiz, G., Bird, M. I., Wurster, C., Quesada, C. A., Ascough, P., Domingues, T., Schrodt, F., Schwarz, M., Feldpausch, T. R., Veenendaal, E., Djangbletey, G., Jacobsen, G., Hie, F., Compaore, H., Diallo, A., & Lloyd, J. (2015). The influence of C3 and C4 vegetation on soil organic matter dynamics in contrasting semi-natural tropical ecosystems. *Biogeosciences*, 12, 5041–5059. <https://doi.org/10.5194/bg-12-5041-2015>
- Scholes, R. J. (2020). The future of semi-arid regions: A weak fabric unravels. *Climate*, 8(3), 43. <https://doi.org/10.3390/cli8030043>
- Serdeczny, O., Adams, S., Baarsch, F., Coumou, D., Robinson, A., Hare, W., Schaeffer, M., Perrette, M., & Reinhardt, J. (2017). Climate change impacts in Sub-Saharan Africa: From physical changes to their social repercussions. *Regional Environmental Change*, 17(6), 1585–1600. <https://doi.org/10.1007/s10113-015-0910-2>
- Serpa, D., Nunes, J. P., Santos, J., Sampaio, E., Jacinto, R., Veiga, S., & Abrantes, N. (2015). Impacts of climate and land use changes on the hydrological and erosion processes of two contrasting Mediterranean catchments. *Science of the Total Environment*, 538, 64–77. <https://doi.org/10.1016/j.scitotenv.2015.08.033>
- Seleshi, Y., & Camberlin, P. (2006). Recent changes in dry spell and extreme rainfall events in Ethiopia. *Theoretical and Applied Climatology*, 83, 181–191. <https://doi.org/10.1007/s00704-005-0134-3>
- Setegn, S. G., Rayner, D., Melesse, A. M., Dargahi, B., & Srinivasan, R. (2011). Impact of climate change on the hydroclimatology of Lake Tana Basin, Ethiopia. *Water Resource Research*, 47, W04511. <https://doi.org/10.1029/2010WR009248>
- Shawul, A. A., Chakma, S., & Melesse, A. M. (2019). The response of water balance components to land cover change based on hydrologic modeling and partial least squares regression (PLSR) analysis in the Upper Awash Basin. *Journal of Hydrology: Regional Studies*, 26, 100640. <https://doi.org/10.1016/j.ejrh.2019.100640>
- Shi, P., Ma, X., Hou, Y., & Li, Q. E. (2013). Effects of land-use and climate change on hydrological processes in the upstream of Huai River, China. *Water Resource*

- Management*, 27, 1263–1278. <https://doi.org/10.1007/s11269-012-0237-4>
- Shiferaw, H., Gebremedhin, A., Gebretsadkan, T., & Zenebe, A. (2018). Modelling hydrological response under climate change scenarios using SWAT model: The case of Ilala watershed, Northern Ethiopia. *Model. Earth Systems and Environment*, 4, 437–449. <https://doi.org/10.1007/s40808-018-0439-8>
- Smetanova, A., Le Bissonnais, Y., Raclot, D., Pedro Nunes, J., Licciardello, F., Le Bouteiller, C., & Follain, S. (2018). Temporal variability and time compression of sediment yield in small Mediterranean catchments: Impacts for land and water management. *Soil Use and Management*, 34(3), 388–403. <https://doi.org/10.1111/sum.12437>
- Stedinger, J. R., & Griffith, V. W. (2008). Flood frequency analysis in the United States: Time to update. *Journal of Hydrologic Engineering*, 13(4), 199–204.
- Strzepek, K., & McCluskey, A. (2006). *District level hydro-climatic time series and scenario analysis to assess the impacts of climate change on regional water resources and agriculture in Africa. Discussion Paper*. Vol. 13. CEEPA
- Subash, N., Harbir, S., Ruane, A., McDermid, S., & Baigorria, G. (2016). Uncertainty of GCM projections under different Representative Concentration Pathways (RCPs) at different temporal and spatial scales—Reflections from 2 sites in Indo-Gangetic Plains of India. In: *the Proceedings of AgMIP 6 Global Workshop*. Le Corum, Montpellier, France, 28–30.
- Taniguchi, M. (1997). *Subsurface hydrological responses to land cover and land use changes*. Springer.
- Taye, M. T., Willems, P., & Block, P. (2015). Implications of climate change on hydrological extremes in the Blue Nile basin: A review. *Journal of Hydrology: Regional Studies*, 4, 280–293. <https://doi.org/10.1016/j.ejrh.2015.07.001>
- Tebaldi, C., Hayhoe, K., Arblaster, J. M., & Meehl, G. A. (2006). Going to the extremes: An inter-comparison of model-simulated historical and future changes in extreme events. *Climatic Change*, 79, 185–211. <https://doi.org/10.1007/s10584-006-9051-4>
- Theobald, D. M., & Hobbs, N. T. (2002). A framework for evaluating land use planning alternatives: Protecting biodiversity on private land. *Ecology and Society*, 6(1). <https://doi.org/10.5751/ES-00379-060105>
- Thomson, A., Calvin, K., Smith, S. J., Kyle, P., Volke, A., Patel, P., Delgado, A. S., Bond-Lamberty, B., Wise, M., Clarke, L., & Edmonds, J. (2011). RCP4.5: A pathway for stabilization of radiative forcing by 2100. *Climate Change*, 109, 77–94. <https://doi.org/10.1007/s10584-011-0151-4>
- Tizora, P., Le Roux, A., Mans, G., & Cooper, A. K. (2018). Adapting the Dyna-CLUE model for simulating land use and land cover change in the Western Cape Province. *South African Journal of Geomatics*, 7(2), 190–203. <https://doi.org/10.4314/sajg.v7i2.7>
- Verburg, P. H. (2010). *The Clue Modelling Framework*. VU Amsterdam, Institute for Environmental Studies. Available: http://www.ivm.vu.nl/en/Images/Exercises_tcm234-284019.pdf. Accessed 23 January 2019. http://www.ivm.vu.nl/en/Images/Exercises_tcm234-284019.pdf
- Verburg, P. H., & Overmars, K. P. (2009). Combining top-down and bottom-up dynamics in land use modeling: Exploring the future of abandoned farmlands in Europe with the Dyna-CLUE model. *Landscape Ecology*, 24(9), 1167–1181. <https://doi.org/10.1007/s10980-009-9355-7>
- Verburg, P. H., & Veldkamp, A. (2004). Projecting land use transitions at forest fringes in the Philippines at two spatial scales. *Landscape Ecology*, 19, 77–98. <https://doi.org/10.1007/s10980-009-9355-7>
- Verburg, P. H., Soepboer, W., Veldkamp, A., Limpiada, R., Espaldon, V., & Mastura, S. S. (2002). Modeling the spatial dynamics of regional land use: The CLUE-S model. *Environmental Management*, 30, 391–405. <https://doi.org/10.1007/s00267-002-2630-x>
- Visser, H., & De Nijs, T. (2006). The map comparison kit. *Environmental Modelling & Software*, 21(3), 346–358. <https://doi.org/10.1016/j.envsoft.2004.11.013>
- Wang, D., Yu, X., Jia, G., & Wang, H. (2019). Sensitivity analysis of runoff to climate variability and land-use changes in the Haihe Basin mountainous area of north China. *Agriculture, Ecosystems & Environment*, 269, 193–203. <https://doi.org/10.1016/j.agee.2018.09.025>
- Williams, J. R. (1975). *Sediment-yield prediction with Universal Equation using runoff energy factor. Present and Prospective Technology for Predicting Sediment Yields and Sources*, ARS-S-40, US Department of Agriculture, Agricultural Research Service, 244–252.
- Woldesenbet, T. A., Elagib, N. A., Ribbe, L., & Heinrich, J. (2017). Hydrological responses to land use/cover changes in the source region of the Upper Blue Nile Basin, Ethiopia. *Science of the Total Environment*, 575, 724–741. <https://doi.org/10.1016/j.scitotenv.2016.09.124>
- Worqlul, A. W., Dile, Y. T., Ayana, E. K., Jeong, J., Adem, A. A., & Gerik, T. (2018). Impact of climate change on streamflow hydrology in headwater catchments of the Upper Blue Nile Basin, Ethiopia. *Water*, 10(2), 120. <https://doi.org/10.3390/w10020120>
- Zhang, P., Liu, Y., Pan, Y., & Yu, Z. (2013). Land use pattern optimization based on CLUE-S and SWAT models for agricultural non-point source pollution control. *Mathematical and Computer Modelling*, 58(3–4), 588–595. <https://doi.org/10.1016/j.mcm.2011.10.061>

Publisher's Note Springer Nature remains neutral with regard to jurisdictional claims in published maps and institutional affiliations.

Springer Nature or its licensor holds exclusive rights to this article under a publishing agreement with the author(s) or other rightsholder(s); author self-archiving of the accepted manuscript version of this article is solely governed by the terms of such publishing agreement and applicable law.